


# Effect of modulating glutamate signaling on myelinating oligodendrocytes and their development—A study in the zebrafish model

Funda Turan<sup>1,2</sup> | Öznur Yilmaz<sup>3</sup> | Lena Schünemann<sup>3</sup> | Tobias T. Lindenberg<sup>1</sup> | Jeshurun C. Kalanithy<sup>3</sup> | Alexander Harder<sup>4</sup> | Shiva Ahmadi<sup>5</sup> | Türker Duman<sup>2</sup> | Ryan B. MacDonald<sup>6</sup> | Dominic Winter<sup>5</sup> | Changsheng Liu<sup>3</sup> | Benjamin Odermatt<sup>1,3</sup> 

<sup>1</sup>Medical Faculty, Institute of Neuroanatomy, University of Bonn, Bonn, Germany

<sup>2</sup>Faculty of Science, Biology Department, Ankara University, Ankara, Turkey

<sup>3</sup>Medical Faculty, Institute of Anatomy and Cell-Biology, University of Bonn, Bonn, Germany

<sup>4</sup>Institute of Physical and Theoretical Chemistry, University of Bonn, Bonn, Germany

<sup>5</sup>Medical Faculty, Institute for Biochemistry and Molecular Biology (IBMB), University of Bonn, Bonn, Germany

<sup>6</sup>Institute of Ophthalmology, University College London, London, UK

## Correspondence

Benjamin Odermatt, Myelination of the CNS, Zebrafish Development, Anatomical Institute, Medical Faculty, University of Bonn, Nussallee 10, 53115 Bonn, Germany. Email: b.odermatt@uni-bonn.de

## Funding information

This work was supported by a NRW-Repatriation grant to B.O. and by the German Research Foundation (DFG)/(INST 1172/37-1 FUGG)

## Abstract

Myelination is crucial for the development and maintenance of axonal integrity, especially fast axonal action potential conduction. There is increasing evidence that glutamate signaling and release through neuronal activity modulates the myelination process. In this study, we examine the effect of manipulating glutamate signaling on myelination of oligodendrocyte (OL) lineage cells and their development in zebrafish (zf). We use the “intensity-based glutamate-sensing fluorescent reporter” (iGluSnFR) in the zf model (both sexes) to address the hypothesis that glutamate is implicated in regulation of myelinating OLs. Our results show that glial iGluSnFR expression significantly reduces OL lineage cell number and the expression of myelin markers in larvae (zfl) and adult brains. The specific glutamate receptor agonist, L-AP4, rescues this iGluSnFR effect by significantly increasing the expression of the myelin-related genes, *plp1b* and *mbpa*, and enhances myelination in L-AP4-injected zfl compared to controls. Furthermore, we demonstrate that degrading glutamate using Glutamate-Pyruvate-Transaminase (GPT) or the blockade of glutamate reuptake by L-trans-pyrrolidine-2,4-dicarboxylate (PDC) significantly decreases myelin-related genes and drastically declines myelination in brain ventricle-injected zfl. Moreover, we found that myelin-specific ClaudinK (CldnK) and 36K protein expression is significantly decreased in iGluSnFR-expressing zfl and adult brains compared to controls. Taken together, this study confirms that glutamate signaling is directly required for the preservation of myelinating OLs and for the myelination process itself. These findings further suggest that glutamate signaling may provide novel targets to therapeutically boost remyelination in several demyelinating diseases of the CNS.

## KEYWORDS

glia, glutamate signaling, iGluSnFR, myelin, oligodendrocyte, OPC, RRID:AB\_476697, zebrafish

Edited by Cristina Ghiani. Reviewed by Marcel Tawk, Joshua Bonkowsky, and Mengsheng Qiu.

This is an open access article under the terms of the Creative Commons Attribution-NonCommercial-NoDerivs License, which permits use and distribution in any medium, provided the original work is properly cited, the use is non-commercial and no modifications or adaptations are made.

© 2021 The Authors. *Journal of Neuroscience Research* published by Wiley Periodicals LLC

## 1 | INTRODUCTION

Axonal myelination is crucial for the mammalian brain to operate correctly. A diversity of factors have been connected with the control of myelination and the differentiation of oligodendroglia. This includes glutamate signaling, which has been shown to affect oligodendrocyte (OL) lineage cells and may be a critical factor for learning-dependent myelination (Kolodziejczyk et al., 2010; Spitzer et al., 2016). Along this line, studies focusing on receptor-dependent glutamatergic mechanisms affecting myelination indicate that oligodendrocyte precursor cells (OPCs) constitute an axon-glia signaling complex influenced by input from electrically active axons through vesicular glutamate release (Bergles et al., 2010; Kukley et al., 2007). Indeed, glutamate release, which broadly occurs in injured or demyelinated axons, is thought to trigger remyelination as soon as OPCs begin to differentiate at the site of injury (De Biase et al., 2010; Etxeberria et al., 2010; Ziskin et al., 2007). All this indicates a tight interplay between OPCs and axons. Many of the signaling factors associating axons to OPCs have been suggested to play a role in the control of OPC migration, proliferation, and differentiation, but the underlying mechanisms still remain widely underexplored (Spitzer et al., 2016).

By using coculture of neurons and OLs, Wake et al. provide evidence that electrical activity, which triggers vesicle release of glutamate from axons, can stimulate calcium signaling within OLs (Wake et al., 2011). Furthermore, this study shows that electrical activity also triggered protein translation of the MBP marker in OL processes and is dependent on glutamate receptor and Fyn kinase functions. The authors elegantly revealed a mechanism for the regulation of myelination in response to local axonal signals (Wake et al., 2011). Fyn kinase plays a crucial role here as an intermediary regulator of local *mbp* translation. In addition to these findings, other reports (Lundgaard et al., 2013; Taveggia et al., 2008; Xiao et al., 2011) demonstrate that myelination is controlled both by activity-dependent and activity-independent machineries.

OLs express both ionotropic and metabotropic glutamate receptors throughout their lineage development (De Biase et al., 2010; Jantzie et al., 2010; Luyt et al., 2006). Remarkably, it has been shown that nonsynaptic glutamate-induced signaling may alter OL lineage cells throughout their differentiation (Chen & Kukley, 2020; Weinreich & Hammerschlag, 1975), where glutamate is supposed to be delivered by an extra-synaptic vesicular machinery and/or by the reversal of glutamate transporter activity (Káradóttir & Attwell, 2007). Interestingly, the concept of nonsynaptic glutamate-induced signaling (Wake et al., 2015) may be confirmed by *in vivo* investigations in the zf model, where electrically active axons have been demonstrated to be preferentially myelinated and their myelin sheaths may be safeguarded (Hines et al., 2015).

Lately, the notion of an axo-myelinic synapse has arisen, and diverse studies indicate a receptor-dependent glutamatergic input from the axon, which is collected at the myelin sheath along the length of an internode (Micu et al., 2018). Whereas, conversely a

### Significance

- Myelination is essential for vertebrate brain function, and glutamate signaling has been associated with the myelination process.
- We modulated glutamate signaling in zebrafish using a novel glutamate reporter (iGluSnFR). When expressed, iGluSnFR drastically diminished oligodendrocyte numbers and myelin marker expression.
- A Glutamate receptor agonist rescues the negative iGluSnFR effects on CNS myelination, as it increases the expression of myelin genes and enhances myelination.
- Pharmacological tools confirm that either degrading glutamate or blocking glutamate reuptake significantly decreases myelin genes and declines myelination.
- Myelin protein expression is significantly decreased in iGluSnFR-expressing zf.
- We demonstrate that glutamate signaling is required for the preservation of myelination and therefore may provide interesting novel targets to therapeutically boost myelination.

functional link relating electrical activity with the metabolic pathway of the OL has also been made (Micu et al., 2018; Saab et al., 2016).

Aside from the progress that has been made to provide mechanistic insights into activity-independent and activity-dependent controls of CNS myelination in many experimental models, a closer examination is still required in this area to elucidate how exactly glutamate pathways modulate the myelination process, which may also be a new way of regulating neuronal plasticity.

In this study, we investigated myelination in the zf model using the recently described (MacDonald et al., 2017) genetic tool—iGluSnFR—an extracellular glutamate sensor under the control of the GFAP promoter. The findings made with the transgenic zf line *Tg(GFAP:iGluSnFR)* were confirmed by directly targeting specific glutamate receptors using pharmacological tools. In summary, the main finding of our study is that a change in extracellular glutamate concentration to a certain extent directly correlates with a decrease or even increase in OPCs as well as mature OLs and myelination.

## 2 | MATERIALS AND METHODS

### 2.1 | Fish husbandry and brain ventricle microinjections

Zebrafish (either sex and mixed strain) were maintained according to national law and under standardized conditions (Westerfield, 2007) at 27.5°C. All fish were bred and maintained naturally (fish-facility water: 550 µS, pH 7.2–7.4; light cycle: 14 hr on and 10 hr off). All zf embryos that developed beyond 24 hr postfertilization (hpf) were

treated with phenylthiourea (PTU; 0.003%, w/v; Sigma) against pigmentation, which was added to Danieau solution. The staging of zfl was performed according to Kimmel et al. (1995).

## 2.2 | Zebrafish strains

Lines used in this study included *Tg(GFAP:GFAP-GFP)* provided by the laboratory of Prof. Uwe Strähle from Karlsruhe Institute of Technology (Chen et al., 2009); *Tg(GFAP:iGluSnFR)* provided by Dr. Ryan MacDonald in the laboratory of Prof. William Harris, University of Cambridge, UK (MacDonald et al., 2017); *Tg(Olig2:dsRed)*, *Tg(CldnK:TdTomato)* and *Tg(CldnK:memTdTomato)* provided by the laboratory of Prof. Catherina G. Becker and the laboratory of Prof. David Lyons (Kucenas et al., 2008; Münzel et al., 2012); *Tg(GFAP:GFAP-GFP)<sup>+/-</sup>*, *Tg(GFAP:iGluSnFR)<sup>+/-</sup>*, *Tg(CldnK:TdTomato)<sup>+/-</sup>*, and *Tg(Olig2:dsRed)<sup>+/-</sup>* zfl were used for scanning two-photon fluorescent imaging. For conventional fluorescence microscopy *Tg(CldnK:memTdTomato)<sup>+/-</sup>*, *Tg(Olig2:dsRed)<sup>+/-</sup>*, and double transgenic *Tg(CldnK:memTdTomato)<sup>+/-</sup>/Tg(GFAP:iGluSnFR)<sup>+/-</sup>* zfl were used.

*Tg(CldnK:memTdTomato)<sup>+/-</sup>* and *Tg(CldnK:memTdTomato)<sup>-/-</sup>* zfl were used for brain ventricle injection, imaging, and qRT-PCR. *Tg(GFAP:iGluSnFR)<sup>+/-</sup>* zfl at 5 and 8 days postfertilization (dpf) and adult zf brain were used for qRT-PCR and Western blot analysis. *Tg(GFAP:iGluSnFR)<sup>+/-</sup>* and WT adult zf brains were isolated according to the protocol by Gupta and Mullins (2010).

We crossed *Tg(CldnK:TdTomato)<sup>+/-</sup>* with *Tg(GFAP:iGluSnFR)<sup>+/-</sup>* zf and analyzed their offspring for OL numbers at 5 dpf by two-photon microscopy. Controls were only *CldnK:TdTomato* positive but GFAP:iGluSnFR-negative zf. As an additional GFP positive control, we used the *Tg(GFAP:GFAP-GFP)<sup>+/-</sup>* line.

Further for this project, we crossed *Tg(Olig2:dsRed)<sup>+/-</sup>* with *Tg(GFAP:iGluSnFR)<sup>+/-</sup>* fish and analyzed their offspring for OPC numbers at 3 dpf by two-photon microscopy. Littermate controls were only *Olig2:dsRed* but not GFAP:iGluSnFR-expressing zf. As an external control, we again used zfl of the *Tg(GFAP:GFAP-GFP)<sup>+/-</sup>* line.

For iGluSnFR PCR genotyping, genomic DNA was isolated from zf tail fin tips. DreamTaq DNA Polymerase (Thermo Scientific (#EP0702)) and following primers were used: forward primer sequence 5'-ATGACACCATCGCTCAGGTGCAGACCTCCG-3' and reverse primer sequence 5'-TAGGTGGCATCGCCCTCGCCCTCGCCG GAC-3' (Sigma-Aldrich) giving a PCR product of 494 bp.

## 2.3 | Brain ventricle microinjections

One microliter volume of 1 mM/L2-amino-4-phosphonobutyric acid (L-AP4) (Thermo Fisher Scientific Corporation), 10 u/ml Glutamate-Pyruvate-Transaminase (GPT) (Sigma) + 50 μM Pyruvate (Sigma), and 1 mM L-trans-pyrrolidine-2,4-dicarboxylate (PDC) (Sigma-Aldrich) were injected individually in the brain ventricle of temporally anesthetized (with Danieau 30% containing 0.160 g/L of MS222) 3 dpf *Tg(CldnK:memTdTomato)<sup>+/-</sup>* and *Tg(CldnK:memTdTomato)<sup>-/-</sup>* zfl with

glass capillaries using standard methods (Gutzman & Sive, 2009). Noninjected zfl and zfl injected with a vehicle (buffer) were used as controls. After injection, fish water was changed daily. At 5 dpf, *Tg(CldnK:memTdTomato)<sup>+/-</sup>* zfl were used to take fluorescence images of the proximal spinal cord region. *Tg(CldnK:memTdTomato)<sup>-/-</sup>* zfl were used for qRT-PCR analysis together with accordingly injected controls. For L-AP4 injection, rescue experiments either *Tg(CldnK:memTdTomato)<sup>+/-</sup>* or *Tg(Olig2:dsRed)<sup>+/-</sup>* crossed to *Tg(GFAP:iGluSnFR)<sup>+/-</sup>* zfl were injected into the ventricle at 3 dpf and imaged at 5 dpf.

## 2.4 | Imaging

For fluorescence scanning microscope two-photon live imaging 3 and 5 dpf zfl were mounted in low melting point (LMP) agarose (2.5%, wt/vol) on a Petri dish lid. Approximately five zfl were covered with 200 μl of agarose containing 0.16 g/L of MS222. The fish were arranged to lay laterally. When the agarose was hardened, the droplet was covered with 30% Danieau containing 0.16 g/L of MS222 (Tricaine).

For pixel intensity fluorescent measurement, images were taken with an Axio Zoom V16 microscope (Zeiss, Germany) or a Nikon AZ100 multi-zoom microscope (Nikon, Germany). The analyst was blinded to the experimental groups during imaging and analysis using Zen (Zeiss) and NIS-Elements (Nikon) software, respectively. Results from both microscopes were comparable but not mixed for analysis.

For the 5 dpf *Tg(CldnK:memTdTomato)* and 3 dpf *Tg(Olig2:dsRed)* zfl, the expression of red fluorescence was evaluated blindly by measuring the pixel intensity of the TdTomato and dsRed fluorescence, in the same region and focal plane of the spinal cord for each zfl, respectively. This was done for drug-injected, vehicle-injected, and uninjected groups as well as double and single transgenic zfl. Images were recorded with an Axio Zoom V16 microscope or Nikon AZ100 multi-zoom microscope (Nikon, Germany) using same illumination and exposure values correspondingly. Image postprocessing without any change in pixel values was carried out with ImageJ software. To quantify CldnK and Olig2 expression, the related pixel intensity was measured in the very same region of interest (ROI) in the spinal cord of all analyzed zfl. The pixel intensity values of each zfl group were averaged and used for statistics.

Images showing OPC and OL numbers were acquired using a LaVision TriM Scope II two-photon point scanning microscope and ImSpector software (LaVision, Bielefeld, Germany). The observer was again blinded for the genotype of the fish before cell counting. Since ventral *Olig2:dsRed<sup>+</sup>* OPCs were extremely dense handicapping the counting process, only dorsal *Olig2:dsRed<sup>+</sup>* OPCs were counted. Dorsally, we could clearly identify and distinguish two cell shapes though. Dorsal migratory *Olig2:dsRed<sup>+</sup>* OPCs could be recognized for their irregular roundish shape, and more mature *Olig2:dsRed<sup>+</sup>* OPCs were recognized on their regular ellipsoid shape (Baumann & Pham-Dinh, 2001; Kirby et al., 2006; Milner et al., 1997; Schmidt et al., 1997; Simpson & Armstrong, 1999; Tsai et al., 2006).

## 2.5 | Statistical analysis

All graphs generated and their statistical analyses were performed using GraphPad Prism version 6.0. software package. All experiments were repeated at least three times ( $N \geq 3$ ) unless otherwise mentioned. In general, N represents the total number of independent experiments and n represents the number zfl or zf used in total.

Data were assayed by one-way ANOVA followed by Bonferroni's multiple comparisons to determine whether there are any statistically significant differences between the means. This was always done for three or more unrelated experimental groups and by unpaired Student's t tests for analysis with only two experimental groups. A value of  $*p < 0.05$  was regarded as statistically significant. Error bars are showing standard error of the mean (SEM).

## 2.6 | (Real-time) quantitative Reverse transcription polymerase chain reaction (qRT-PCR)

Single adult zf brains or 25 frozen 5 dpf zfl were homogenized in Trizol TriReagent® (Thermo Fisher Scientific Corporation), where RNA was then precipitated with isopropanol, eluted, and dissolved in RNase-free H<sub>2</sub>O. Total RNAs' quantity was assessed with a Qubit Fluorometer (Invitrogen) Spectrophotometer, and were stored at -80°C until further use. cDNAs were synthesized using 2 µg RNA, 4 µl iScript Supermix (BioRAD), and RNase-free H<sub>2</sub>O (BioRAD) in a total reaction mixture volume of 20 µl.

The zf-specific intron spanning forward (FP) and reverse (RP) primers were as follows: for  $\beta$ -actin: GCCAACAGAGAGAAGATG (FP) and GCGTAACCCTCATAGATG (RP); for *ef1a*: GGAGTGATCTCTC AATCTTG (FP) and CTCCTTCTCGAACTTCTC (RP); for *plp1b*: CAGGAATCACCCTTCTTG (FP) and GAACCTAGCAACGGATTC (RP); and for *mbpa*: CTGGGCAGAAAGAAGAAG (FP) and GATGACCACGA AATGAAC (RP). The following internal quenched fluorescent probes were used and their sequences are cited below: actb1 probe ST01473661: [6FAM]ACCATCACCAGAGTCCATCACAAAT[BHQ1]; *eef1a111* probe ST01907165: [6FAM]TCTCTTGTCGATTCCACC GCA[BHQ1], *plp1b* probe ST01473662: [HEX]CCACCACCTACAA CTACGCTATTCT[BHQ1], and *mbpa* probe ST01907116: [HEX] CTCCTCCGAAGAACCTGCTGAT[BHQ1].

Reaction mixes (20 µl) were assembled in a 96-well plate as follows: 10 µl Polymerase Master Mix (Thermo Scientific Corporation), 0.4 µl of forward primer (10 mM FP), 0.4 µl of reverse primer (10 mM RP), 0.2 µl internal probe (25 µM), 7 µl dd H<sub>2</sub>O, and 2 µl cDNA (50 pg/µl). The qRT-PCRs were carried out using a CFX96 Real-Time System C1000 Thermal Cycler (Bio Rad). After denaturation at 95°C for 7 min, 40 PCR cycles were performed—5 s at 95°C and 30 s at 60°C. All qRT-PCR data were normalized to the reference genes and scaled to the average, hence generating calibrated normalized relative quantities (CNRQ) (Hellemans et al., 2008) using qbase+ software (Biogazelle). The standard curve and primer efficiency for *plp1b*, *mbpa*, and  $\beta$ -actin as well as *ef1a* as reference genes were preliminarily determined in our laboratory (Nagarajan et al., 2020).

## 2.7 | Western blotting

Methods for Western blot analysis were similar for all experiments. Single adult zf brains or 25 zfl were homogenized using pellet pestle in a standard RIPA buffer (Thermo Scientific) plus protease inhibitor cocktail (Roche), centrifuged at 4°C for 20 min. Supernatant was taken and measured for protein concentration using Pierce BCA Protein Assay Kit (Thermo Fisher 23225). Fifty micrograms for zfl and 1 µg for adult brain protein was then diluted in Laemml buffer and was loaded in each lane on a 4%–15% gradient mini-protean TGX gel (BioRad) and, after running electrophoresis separation, was then transferred to a PVDF membrane (Bio-Rad) using Trans Turbo blot (BioRad). Protein-loaded PVDF membranes were blocked in 1x TBS with 0.1% Tween 20 and 5% milk powder (1x TBS: 150 mM NaCl, 10 mM Tris-HCl, pH 8.0) for 2 hr and then incubated in primary antibody diluted in blocking buffer overnight at 4°C (custom-made anti-CldnK (*D. rerio* CldnK Aa 200-216) (Thermo Scientific) (1:10.000), custom-made anti-36K (*D. rerio* flj13639 Aa 302-320) (Thermo Scientific) (1:10.000) (Nagarajan et al., 2020), anti-EGFP (Clontech-632381) (1:2.000), and anti- $\beta$ -actin (Sigma-Aldrich-A2228—RRID:AB\_476697) (1:50.000)).

The immunoreactive bands were detected using enhanced chemiluminescence (SuperSignal West femto chemiluminescent substrate; Pierce). The intensity of the bands was measured using ImageJ software. Using ImageJ, the noise background was subtracted from each corresponding band. The relative intensity of each band was then calculated (in relation to  $\beta$ -actin as loading control, this was done for each protein of interest) separately. Finally, a membrane/experiment-related comparison factor was calculated based on the average  $\beta$ -actin bands intensities. The latter was then used before averaging the protein of interest relative intensities from different experiments.

## 2.8 | Immunohistochemistry

For paraffin sections, zfl or adults were anesthetized by immersion in MS222 (1:1.000), followed by immersion in 4% formalin in PBS overnight an embedded in paraffin. Zf tissue sections were deparaffinized using a serial washing with xylol, ethanol, and PBS, subjected to heat- induce antigen retrieval protocol (10 mM Tris-EDTA buffer (10 mM Tris base, 1 mM EDTA solution, 0.05% Tween 20, pH 9.0) at 80°C for 1 hr) permeabilized with 1x PBS + 0.05% Tween 20 for 10 Minutes at RT, treated with endogenous peroxidase (10% Methanol + 1% H<sub>2</sub>O<sub>2</sub> in 1x PBS), blocked with 10% NGS + 2% BSA + 0.1% Triton X-100 in 1XPBS, and then treated with primary antibodies at following dilutions: the anti-PCNA (dilution 1:2.000, Abcam #2426 AB\_18197, host:Rabbit), custom-made CldnK (dilution 1:300), custom-made 36K (dilution 1:200, Thermo Scientific #QPE0580 host:Rabbit), *mbpa* (dilution 1:200, Thermo Scientific PA1-46447 AB\_2140360; Host:Guinea Pig), custom-made CC3 (dilution 1:200, cell signaling #9661, host:Rabbit), and anti-EGFP (Takara Clontech 632380) 1:1.000, and treated with the

corresponding biotinylated goat anti-rabbit secondary antibodies (dilution 1:750). Slides were imaged using conventional upright light microscopy (Nikon Eclipse).

### 3 | RESULTS

To investigate the role of glutamate in CNS-myelin regulation, we used four different breeds of fish: first, a double transgenic line expressing iGluSnFR under the GFAP promoter and the red fluorescent cytoplasmatic TdTomato protein under the ClaudinK (CldnK) promoter. Second, a double transgenic line expressing iGluSnFR under the GFAP promoter and the red fluorescent cytoplasmatic DsRed protein under the Olig2 promoter. Third and fourth, their siblings expressing either TdTomato or DsRed under the CldnK or Olig2 promoter, respectively, but not expressing the green fluorescent iGluSnFR.

We started to investigate the possible relationship between the extracellular amount of glutamate—conveyed to us by the green iGluSnFR reporter fluorescence intensity—and the corresponding status of adjacent CNS myelination—demonstrated by the red myelin reporters. However, we found that the iGluSnFR fluorescence intensity was not changing with time—meaning not reporting any changes in extracellular glutamate concentration within the developing spinal cord of the zf. The iGluSnFR fluorescence intensity was not changing even after stimulation of the spinal cord. We speculated that glutamate levels were so high, that it is completely saturating the iGluSnFR reporter in this tissue. Second, we found that the expression of the iGluSnFR reporter under the GFAP promoter modified OL numbers in the zf spinal cord. Importantly the transgenic zebrafish line *Tg(GFAP:iGluSnFR)* is expressing the fluorescent glutamate sensor iGluSnFR on the surface of GFAP<sup>+</sup> (radial)-glia cells. Thus, the sensor's glutamate-binding domain is exposed to the extracellular space, where we speculated it might buffer away some extracellular—synaptically released—glutamate in a sponge-like fashion and diminish free glutamate levels. To ensure proper iGluSnFR reporter protein in our fish line, we performed a DNA sequencing of the coding region of the reporter performing genomic PCR in three independent adult fish, and found no DNA sequence mutation when compared to the formerly published UAS:iGluSnFR.zf1 sequence (addgene Plasmid #108356; data not shown).

Upon initial screening, we immediately noticed a difference in the number of TdTomato<sup>(+)</sup> OLs in the iGluSnFR-expressing zfl (Figure 1a). There are less red-labeled OLs in the dorsal or ventral spinal cord compared to both iGluSnFR neg<sup>(-)</sup> and GFAP:GFAP-GFP pos<sup>(+)</sup> zfl controls. We found a significant reduction of total labeled OLs in iGluSnFR-expressing zfl at 5 dpf. They were reduced by ~45% and ~50% compared to non-iGluSnFR-expressing siblings and external controls, respectively;  $48 \pm 15$  cells in iGluSnFR<sup>(+)</sup> compared to  $88 \pm 14$  in iGluSnFR<sup>(-)</sup> siblings ( $***p < 0.0001$ ) and  $95 \pm 12$  in external GFAP-GFP<sup>(+)</sup> controls ( $***p < 0.0001$ ; one-way ANOVA:  $F = 91.47$ ;  $df = 80$ ; Figure 1b). This reduction was not restricted to either the dorsal or ventral spinal cord OLs. Both spinal cord regions

showed a significant decrease in OL numbers when the fish expressed iGluSnFR. However, the decrease was larger in the dorsal spinal cord. Here, the OL number was reduced by ~67% and ~70% compared to siblings and external controls, respectively;  $8 \pm 5$  cells compared to  $24 \pm 6$  in siblings ( $***p < 0.0001$ ) and  $26 \pm 5$  in external controls ( $***p < 0.0001$ ; one-way ANOVA:  $F = 80.49$ ;  $df = 80$ ; Figure 1c). In the ventral spinal cord region, this reduction amounted only to ~35% and ~40% compared to siblings and external control;  $39 \pm 10$  cells in iGluSnFR<sup>(+)</sup> zfl compared to  $60 \pm 11$  in iGluSnFR<sup>(-)</sup> siblings ( $***p < 0.0001$ ) and  $65 \pm 10$  in external GFAP-GFP<sup>(+)</sup> controls ( $***p < 0.0001$ ) (one-way ANOVA;  $F = 49.28$ ;  $df = 80$ ; Figure 1d).

In summary, extracellular iGluSnFR expression under the GFAP promoter caused a significant loss of CldnK:TdTomato<sup>(+)</sup> OLs in 5 dpf zfl. This loss was particularly high in the dorsal spinal cord. Whereas, GFAP-GFP expression instead of iGluSnFR under the same GFAP promoter as a control produces similar numbers of CldnK:TdTomato<sup>(+)</sup> OLs in 5 dpf zfl as compared to iGluSnFR<sup>(-)</sup> siblings. Because iGluSnFR is attached to the outer membrane of GFAP<sup>+</sup> cells and GFAP-GFP is a cytosolic fibrillary fusion protein, their expression patterns (middle column in Figure 1a) appear different on a small intracellular scale. Their overall cell distribution within the zfl, however, is identical.

Next we looked to determine how earlier developmental stages of the OL lineage cells were influenced by the iGluSnFR expression. Therefore, we quantified dorsal-migrated Olig2:dsRed<sup>(+)</sup> cells in the spinal cord of 3 dpf zfl in two-photon Z-stack images (Figure 2a). The Olig2 promoter is active in OL lineage cells and motor neurons originating from pMN progenitors (Zannino & Appel, 2009). Motor neurons do not migrate dorsally though and thus remain only in the ventral spinal cord (Figure 2b—within yellow borders). For this reason, only the dorsally migrated OPCs were counted in our experiment. We found a significant reduction of these dorsal-migrated Olig2:dsRed<sup>(+)</sup> cells in iGluSnFR-expressing fish. This diminution reached ~35% and ~30% compared to iGluSnFR<sup>(-)</sup> siblings ( $***p < 0.001$ ) and external GFAP-GFP<sup>(+)</sup> control zfl ( $***p < 0.001$ ), respectively (Figure 2c). In iGluSnFR<sup>(+)</sup> zfl, we found on average  $106 \pm 32$  cells compared to  $164 \pm 25$  in iGluSnFR<sup>(-)</sup> siblings ( $***p < 0.001$ ) and  $151 \pm 46$  cells in external GFAP-GFP<sup>(+)</sup> controls ( $***p < 0.001$ ; one-way ANOVA:  $F = 13.66$ ;  $df = 49$ ; Figure 2c). This reduction of OPCs was not as obvious as the reduction in CldnK:TdTomato<sup>(+)</sup> OL cells (Figure 1a), but could nevertheless easily be observed in microscopic images solely by eye (Figure 2a).

Importantly, we also found a significant decrease in cell numbers of more immature dorsal migratory Olig2:dsRed<sup>(+)</sup> OPCs with irregular or roundish shape (green boxes in example Figure 2b), which was in the range of the reduction of total dorsal OPCs. This reduction peaked at the highest value of ~34% and ~31% compared to siblings ( $***p < 0.001$ ) and external control ( $***p < 0.001$ ), respectively;  $101 \pm 29$  cells compared to  $154 \pm 24$  in siblings and  $147 \pm 43$  in external controls ( $***p < 0.001$ ; one-way ANOVA:  $F = 13.75$ ;  $df = 50$ ; Figure 2d).

As shown in the graph in Figure 2e, for the mature dorsal OPCs however, we only found a significant difference between

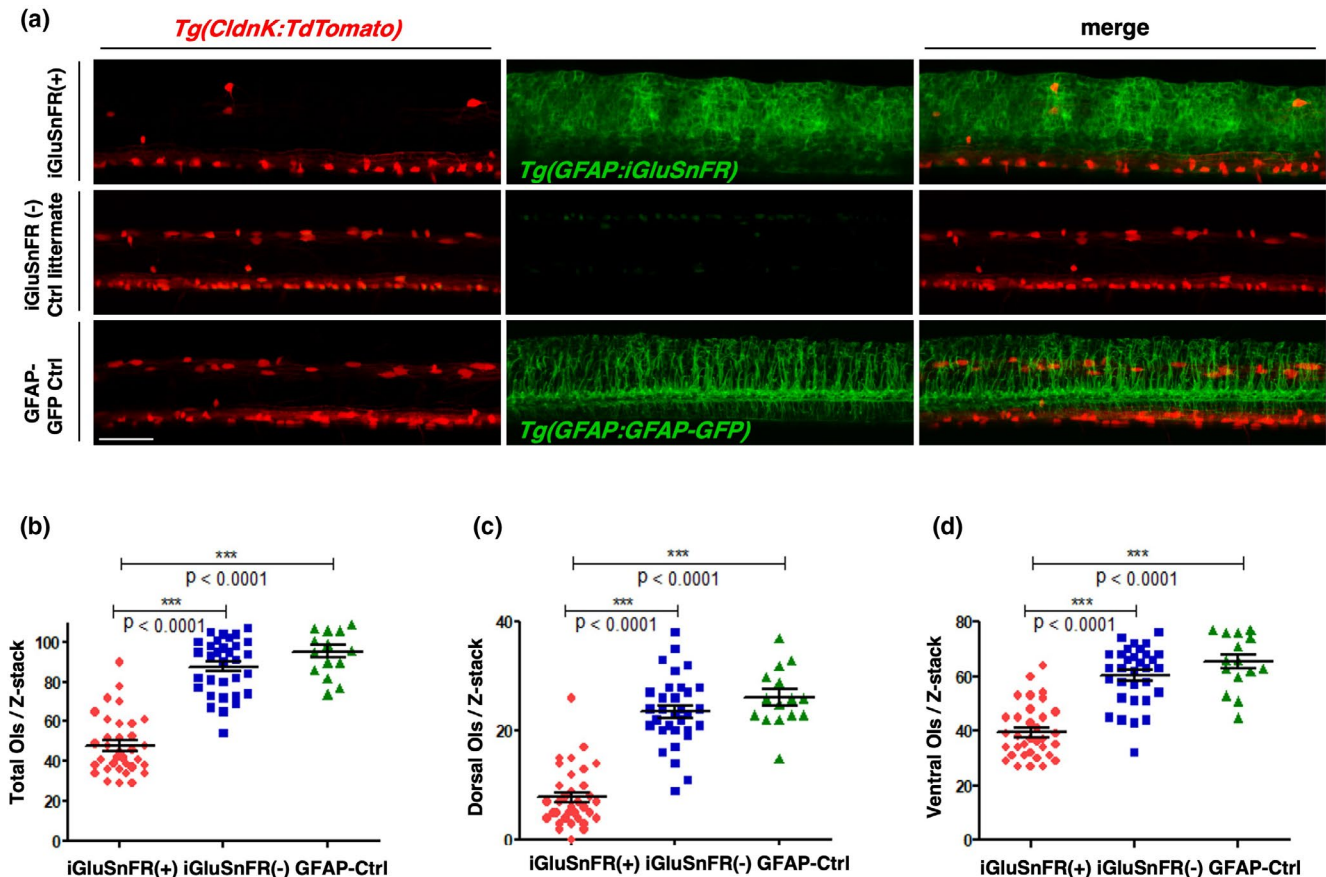


**FIGURE 1** iGluSnFR expression under the GFAP promoter reduces significantly the myelinating oligodendrocyte number in zebrafish. The number of ClaudinK<sup>(+)</sup> OLs was reduced in iGluSnFR-expressing zebrafish larvae at 5 dpf. (a) Z-projections of proximal spinal cord regions in lateral view obtained by two-photon in vivo microscopy. The top row shows double transgenic fish expressing GFAP:iGluSnFR and ClaudinK:TdTomato. In the second row, iGluSnFR<sup>(-)</sup> littermate controls are shown. The third row shows images of double transgenic fish expressing GFAP:GFAP-GFP and ClaudinK:TdTomato. Red and green channels are presented in the first and second image of each row, respectively. The third right image is a merge of both channels. Fish that express iGluSnFR appear to have reduced numbers of red-labeled OLs. Scale bar: 50  $\mu$ m. (b–d) Quantification of cell numbers of total (b), dorsal (c), and ventral (d) OLs. The number of OLs was quantified by counting TdTomato<sup>(+)</sup> cells per Z-stack. Each Z-stack had the same dimensions in x, y, and z and was obtained from approximately the same region within the fish. The total number of OLs was significantly reduced in iGluSnFR-expressing fish (red dots) (b). Both regions (dorsal and ventral) show significant OL loss (c, d). However, the percentage decrease in dorsal OL numbers was higher (c). The iGluSnFR<sup>(-)</sup> (blue squares) and GFAP-Ctrl (green triangles) larvae do not show any significant difference between each other. Data were analyzed by one-way ANOVA followed by Bonferroni's multiple comparisons. \*\*\* indicates a  $p$ -value < 0.001; (b)  $F = 91.47$ ;  $df = 80$ ; (c)  $F = 80.49$ ;  $df = 80$ ; (d)  $F = 49.28$ ;  $df = 80$ . Dot plots show arithmetic mean  $\pm$  standard deviation.  $N = 3$ ,  $n$  in iGluSnFR<sup>(+)</sup> = 34;  $n$  in iGluSnFR<sup>(-)</sup> = 32 and  $n$  in GFAP-Ctrl = 15

iGluSnFR-expressing fish and the littermate controls (\*\* $p < 0.01$ ). Here we noticed a reduction by ~52% when iGluSnFR was expressed (\*\* $p < 0.01$ ; one-way ANOVA:  $F = 5.413$ ;  $df = 49$ ; Figure 2e). However, the total number of rather mature OPCs with regular ellipsoid shape (red boxes in example Figure 2b) was comparably modest at 3 dpf and their standard deviation relatively high;  $5 \pm 5$  cells compared to  $10 \pm 4$  in siblings and  $9 \pm 6$  cells in the external GFAP-GFP controls.

In conclusion, at 3 dpf, we observed a significant diminution in immature, migratory OPCs, which make up the majority of OL lineage cells at this time of development in comparison to both controls. The degree of reduction was not as high as the reduction in mature CldnK:TdTomato<sup>(+)</sup> OLs at 5 dpf, but as mentioned before in the *Tg(Olig2:dsRed)* zf line, we could only count that subset of OPCs that had already migrated dorsally.

Even though the decrease in Olig2:dsRed<sup>(+)</sup> cells was obvious, we quantified the red fluorescence level (pixel intensity) of the proximal spinal cord of each 3 dpf zfl (Figure 3a, three replicates for each). In iGluSnFR-expressing fish, we see a significant reduction in red fluorescence intensity reaching ~35% compared to littermate controls (\*\* $p < 0.001$ ; unpaired two-tailed  $t$  test;  $t = 9.208$ ; Figure 3b). This is precisely the same level of reduction as found for dorsal OPC numbers (Figure 2).

Confirming this result, we found that the expression of red fluorescent mem-tdTomato under the CldnK promoter as a marker for myelination is significantly decreased at 5 dpf (\*\* $p < 0.001$ ; unpaired two-tailed  $t$  test;  $t = 4.597$ ; Figure 3c,d) in iGluSnFR<sup>(+)</sup>-expressing zfl compared to control siblings. This finding confirms a significant decrease (\*\* $p < 0.0001$ ) in

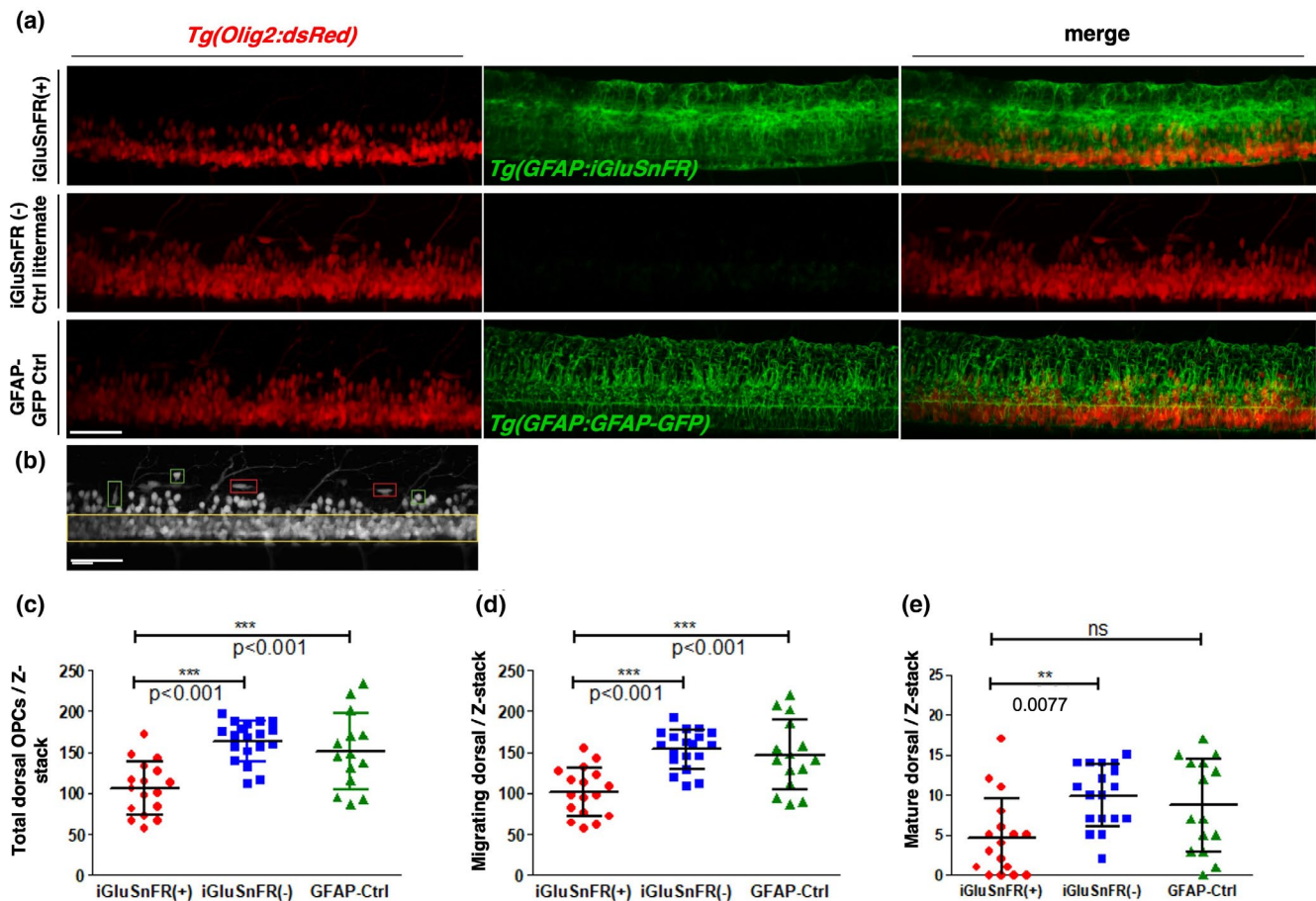


**FIGURE 2** The number of  $Olig2^{(+)}$  OPCs is reduced in iGluSnFR-expressing zebrafish at 3 dpf. (a) Z-projections of proximal spinal cord regions in lateral view obtained by two-photon microscopy. The top row shows double transgenic animals expressing  $Olig2:dsRed$  and  $GFAP:iGluSnFR$ . In the middle row,  $iGluSnFR^{(-)}$  littermate controls are shown. The bottom row shows images of double transgenic larvae fish expressing  $Olig2:dsRed$  and  $GFAP:GFAP-GFP$ . These  $GFAP:GFAP-GFP$  fish serve as an external control for the overexpression of fluorescent proteins under the  $GFAP$  promoter, in general. Red and green channels are presented in the left and middle image of each row, respectively. The third right image shows a merged of both channels. A clear difference in  $dsRed^{(+)}$  cell numbers (OPCs) is already visible by eye. Larvae fish that express iGluSnFR noticeably appear to have reduced numbers of labeled OPCs. Scale bar: 50  $\mu m$ . (b) Example b/w image of a  $Tg(Olig2:dsRed)$  zebrafish larvae taken at a comparable spinal cord region like in (a) to demonstrate the ventral region of the spinal cord in between the two yellow lines as well as some typical more roundish or ventral-dorsal elongated “migratory OPCs” (green squares) and some typical “more mature OPCs” with a rather horizontal flat/ellipsoid shape (red squares). Scale bar: 20  $\mu m$ . (c–e) Quantification of the number of dorsal OPCs. The number of dorsal OPCs was quantified by counting all  $dsRed^{+}$  cells above the upper ventral boarder (yellow line) per Z-stack. Each Z-stack had the same dimensions in x, y, and z and was obtained from approximately the same region in the fish. The total number of dorsal OPCs was significantly reduced in iGluSnFR-expressing fish (c). For migratory OPCs (green squares in b), we also observed a significant reduction in iGluSnFR-expressing fish compared to both controls (d). Concerning the more mature OPCs (red squares in b), we only found a significant reduction when comparing the iGluSnFR-expressing fish with  $iGluSnFR^{(-)}$  littermate controls (e). The  $iGluSnFR^{(-)}$  and  $GFAP-Ctrl$  larvae do not show any significant difference between them. Data were analyzed by one-way ANOVA followed by Bonferroni’s multiple comparisons. \*\*\* indicates a  $p$ -value < 0.001. \*\* indicates a  $p$ -value < 0.01; (c)  $F = 13.66$ ;  $df = 49$ ; (d)  $F = 13.75$ ;  $df = 50$ ; (e)  $F = 5.413$ ;  $df = 49$ . Dot plot graphs show arithmetic mean  $\pm$  standard deviation.  $N = 3$ ,  $n$  in  $iGluSnFR^{(+)}$  = 17;  $n$  in  $iGluSnFR^{(-)}$  = 19 and  $n$  in  $GFAP-Ctrl$  = 14

myelinating OLs correlating with the OL number decrease seen in Figure 1 before.

In conclusion, spinal cord OPCs and OL number are significantly reduced in iGluSnFR-expressing zfl at 3 as well as at 5 dpf, respectively. To validate this observation for the whole zfl, we aimed to further estimate the mRNA expression level of the myelin-related genes *mbpa* and *plp1b* in iGluSnFR-expressing zfl compared to littermate controls. As shown in Figure 4a, our qRT-PCR results confirmed that

these myelin-related genes are significantly decreased in iGluSnFR-expressing zfl at 5 dpf (*mbpa*:  $*p = 0.0473$ ;  $t = 1.984$  and *plp1b*:  $**p = 0.0023$   $t = 4.378$ ; unpaired two-tailed  $t$  test; Figure 4a). At the same time, there was no significant difference in the expression of the housekeeping genes  $\beta$ -actin and *elf1a* in these iGluSnFR-expressing 5 dpf zfl compared to their littermate controls ( $\beta$ -actin:  $p = 0.5124$ ;  $t = 0.6962$  and *elf1a*:  $p = 0.3307$ ;  $t = 1.058$ ; unpaired two-tailed  $t$  test).

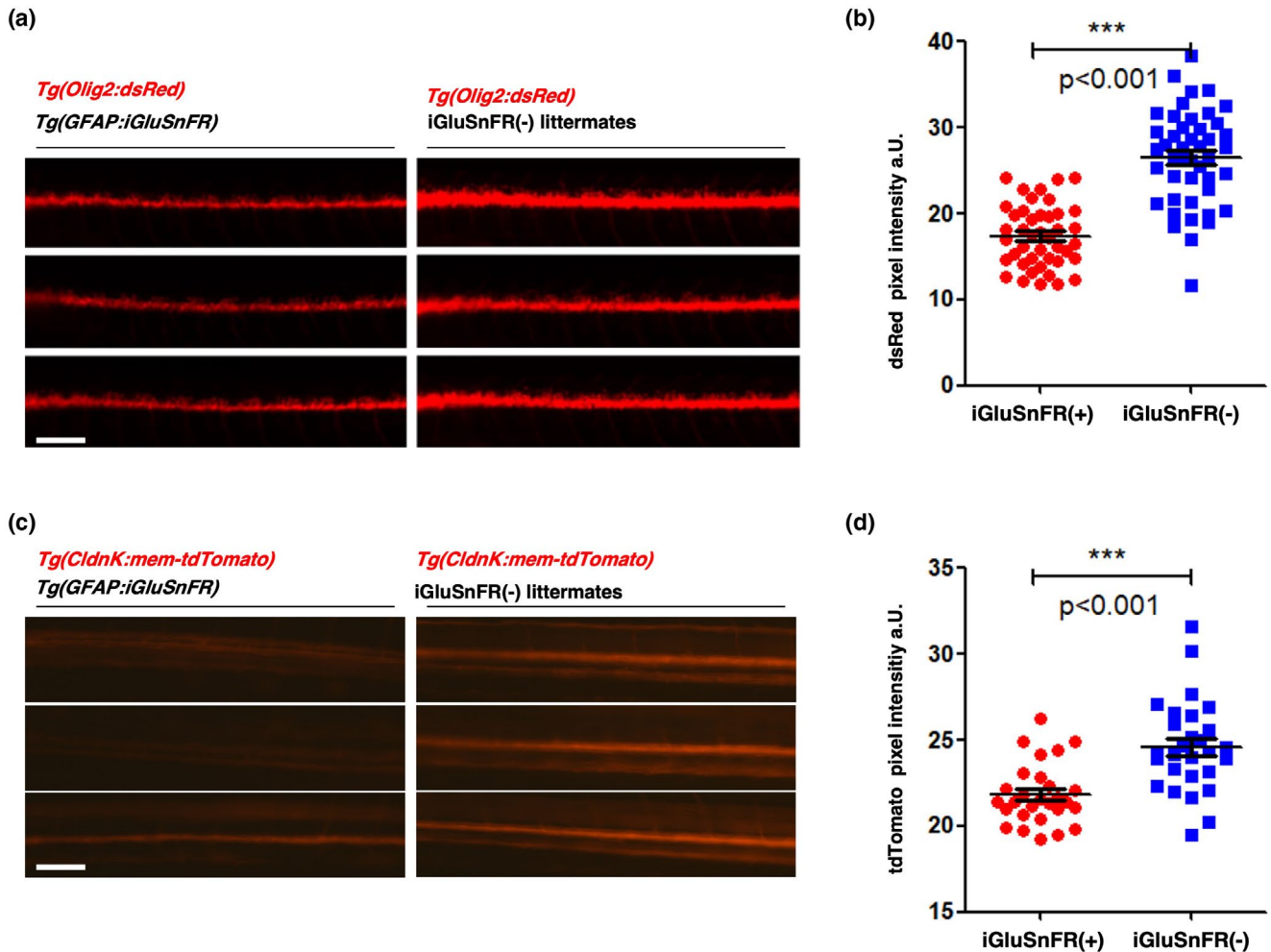


**FIGURE 3** Analysis of fluorescent OPC and myelin reporter intensities. The finding that iGluSnFR-expressing zebrafish larvae shows a reduction in dorsal Olig2<sup>(+)</sup> cells at 3 dpf (see Figure 2c) could be replicated and extended to ventral cells of the proximal region of the spinal cord by examination of global Olig2:dsRed fluorescence intensities. (a) Low-resolution epi-fluorescence microscopic images of proximal zebrafish spinal cords in lateral view. Olig2:dsRed and GFAP:iGluSnFR double transgenic fish at 3 dpf on the left and only Olig2:dsRed-expressing siblings are depicted on the right (red channel only). Scale bar: 100  $\mu$ m. (b) Quantification of relative Olig2:dsRed fluorescence intensities as a parameter for cell numbers. Data were analyzed by an unpaired two-tailed *t* test. \*\*\* indicates a *p*-value < 0.001; *t* = 9.208. The dot plot graph shows the arithmetic mean  $\pm$  standard deviation. *N* = 3, *n* in iGluSnFR<sup>(+)</sup> = 43 (red dots), *n* in iGluSnFR<sup>(-)</sup> = 45 (blue squares). (c) Expression of CldnK is decreased in iGluSnFR<sup>(+)</sup> larvae at 5 dpf compared to controls. CldnK linked to red fluorescent expression in *Tg(CldnK:mem-TdTomato)* zfl is considerably high in control littermate larvae which do not express iGluSnFR (right) compared to *Tg(CldnK:mem-TdTomato)* *Tg(GFAP:iGluSnFR)* double transgenic larvae (left) at 5 dpf. (d) As a marker for myelination, the relative expression of ClaudinK:mem-TdTomato fluorescence intensities was measured and showed a considerable decrease in iGluSnFR<sup>(+)</sup> larvae versus littermate iGluSnFR<sup>(-)</sup> controls (blue squares). The fluorescence level (pixel intensity) of the proximal spinal cord of each larva was quantified within the same area and same microscopy settings. Dot plot graphs show averaged values of pixel density areas (mean  $\pm$  StDev) Data were analyzed by an unpaired two-tailed *t* test. *p*-Values are significant \*\*\**p* < 0.001; *t* = 4.597; *N* = 2 independent experiments with a total of 56 larvae (*n*)

To further validate this observation, we evaluated the expression levels of myelin-related genes, *mbpa* and *plp1b*, using qRT-PCR at 8 dpf. We found that *mbpa* and *plp1b* are significantly decreased in iGluSnFR-expressing zfl at the age of 8 dpf as well (data not shown). In the same line of evidence, we found by Western blot analysis, that the expression of the myelin-related proteins CldnK and 36K is significantly decreased in iGluSnFR-expressing 5 dpf zfl as shown in Figure 5a,c, compared to control siblings (CldnK: \*\*\**p* = 0.0001; *t* = 4.500 and 36K: \**p* = 0.0117; *t* = 2.897; unpaired two-tailed *t* test). This finding agrees with the immunostaining data

of the myelin-related protein Mbpa in the brain and spinal cord of 5 dpf zfl (Figure S4a,b respectively), where specific mbpa staining was diminished in zfl-expressing iGluSnFR compared to littermate controls.

To further confirm that glutamate signaling is demanded for the general regulation of myelination, we examined the effect of iGluSnFR expression in adult zf brain compared to non-iGluSnFR-expressing wildtype (WT) fish. For this we were using qRT-PCR, and found again that mRNA expression of the myelin-related genes *mbpa* and *plp1b* was significantly decreased in iGluSnFR-expressing



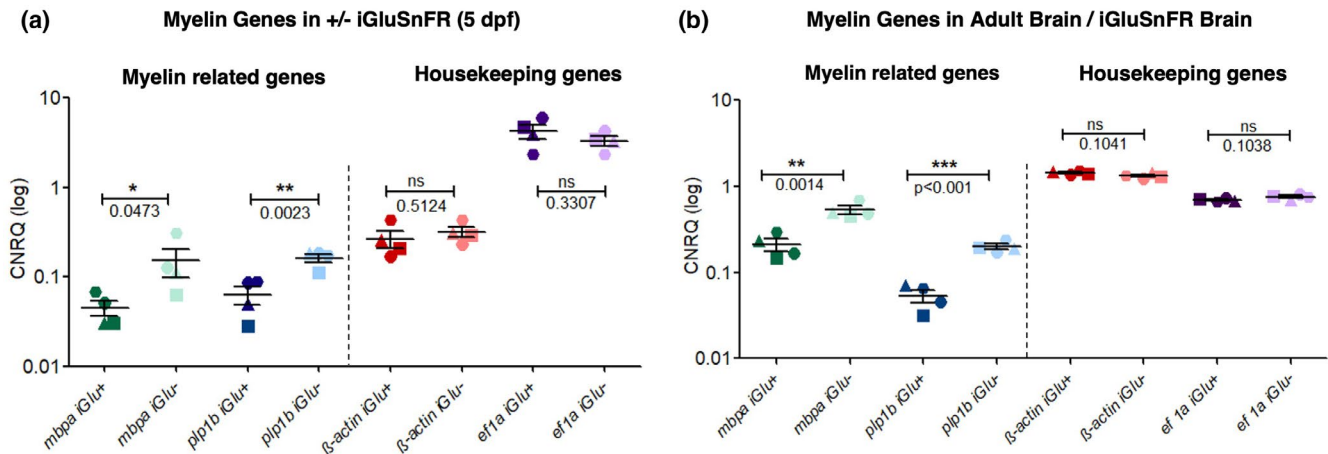


**FIGURE 4** mRNA expression of myelin-related genes is significantly decreased in iGluSnFR-expressing 5 dpf zebrafish larvae and adult brains. (a) Logarithmic representation of calibrated normalized relative quantity (CNRQ) values showing mRNA quantification of the myelin genes *mbpa*:  $0.045 \pm 0.009$  versus  $0.152 \pm 0.053$  green;  $p = 0.0473$ ;  $t = 1.984$  and *plp1b*:  $0.06 \pm 0.01$  versus  $0.16 \pm 0.01$ ; blue;  $p = 0.0023$ ;  $t = 4.378$  together with the housekeeping genes  $\beta$ -actin:  $0.27 \pm 0.06$  versus  $0.32 \pm 0.04$ ; red;  $p = 0.5124$ ;  $t = 0.6962$  and *ef1a*:  $4.23 \pm 0.77$  versus  $3.32 \pm 0.40$ ; purple;  $p = 0.3307$ ;  $t = 1.058$ ; isolated from iGluSnFR-expressing 5 dpf larvae in comparison to iGluSnFR<sup>(-)</sup> siblings, respectively. mRNA levels were normalized against  $\beta$ -actin and *ef1a* housekeeping gene expression. Each color (dark for iGluSnFR<sup>(+)</sup> and light for iGluSnFR<sup>(-)</sup>) represents a different gene, each shape represents an independent experiment. Data were analyzed by an unpaired two-tailed *t* test; \* indicates a *p*-value < 0.05; \*\* indicates a *p*-value < 0.01; \*\*\* indicates a *p*-value < 0.001. The housekeeping genes  $\beta$ -actin and *ef1a* do not show any significant difference whether iGluSnFR is expressed (+) or not (-). Values show mean  $\pm$  SEM.  $N = 4$  independent experiments as indicated by different shapes. (b) mRNA expression of myelin-related genes is decreased significantly in iGluSnFR-expressing adult fish brain compared to WT littermate brain. As for the larvae fish in (a) logarithmic representation of CNRQ values showing mRNA quantification of the following genes: *mbpa*:  $0.21 \pm 0.03$  versus  $0.53 \pm 0.05$ ;  $p = 0.0014$ ;  $t = 4.860$  *plp1b*:  $0.05 \pm 0.009$  versus  $0.20 \pm 0.01$ ;  $p < 0.001$ ;  $t = 8.281$ ;  $\beta$ -actin:  $1.44 \pm 0.03$  versus  $1.33 \pm 0.04$ ;  $p = 0.1041$ ;  $t = 1.914$  and *ef1a*:  $0.69 \pm 0.02$  versus  $0.75 \pm 0.02$ ;  $p = 0.1038$ ;  $t = 1.916$ . This time though isolated from iGluSnFR-expressing adult fish brain compared to control WT littermate brains, and not from larvae fish. mRNA levels were normalized against  $\beta$ -actin and *ef1a* housekeeping genes expression. Both housekeeping genes do not show any significant difference when iGluSnFR is expressed compared to WT brain controls. Again, each color represents a different gene, each shape represents an independent experiment. Data were evaluated by *t* test. Values show mean  $\pm$  SEM.  $N = 4$  independent experiments as indicated by different shapes

adult zf brains compared to WT (*mbpa*: \*\* $p = 0.0014$ ;  $t = 4.860$  and *plp1b*: \*\*\* $p < 0.001$ ;  $t = 8.281$ ; unpaired two-tailed *t* test; Figure 4b). Supporting this finding, the expression of myelin-related proteins CldnK, 36K, and *Mbpa* was also decreased significantly in iGluSnFR-expressing adult zf brains compared to WT brains as shown in our Western blot results (CldnK: \*\*\* $p < 0.0001$ ;  $t = 5.522$ ; 36K: \*\* $p = 0.0094$ ;  $t = 2.848$  and *Mbpa*: \*\*\* $p = 0.0007$ ;  $t = 4.496$ ; unpaired two-tailed *t* test; Figure 5b,c). No significant difference in housekeeping gene expression could be detected in iGluSnFR-expressing adult zf brains compared to controls. Immunostaining data of the myelin-related proteins CldnK and 36K in adult zf brain (Figure S5a–c) again showed that CldnK and 36K expressions were diminished in zf-expressing iGluSnFR compared to littermate controls. As expected, there was a strong signal seen using an anti-EGFP antibody to detect iGluSnFR in these adult zf brains, but not in WT zf control brains (Figure S5f), confirming the specificity of our immunohistochemical analysis as well as the genotype of the used zfl. Furthermore, to ascertain that iGluSnFR is undoubtedly expressed in the selected iGluSnFR<sup>(+)</sup> zfl and adult zf brains, we checked its protein expression using this anti-EGFP antibody to detect iGluSnFR by Western blot. We found, as expected, that iGluSnFR (at ~70 kDa) was both expressed in the respective adult brains and (with a double

band) in 5 dpf zfl, but not in iGluSnFR-negative (PCR negative, non-fluorescent) controls (Figure S1).

In agreement with our hypothesis, these findings indicate that the OL number and myelin-reducing effect of iGluSnFR expression in zfl by potential glutamate buffering can be seen in adult zf as well. Consequently, our data suggest that glutamate signaling might regulate the OPC/OL proliferation and differentiation also at long term, and thus the lasting myelination state of the CNS. Although neuronal activity may not be essential for myelination (Lundgaard et al., 2013), it is still plausible that the release of glutamate may fortify OPCs to differentiate into myelinating OLs that may then recover lost function (Hines et al., 2015; Mensch et al., 2015). Or that glutamate possibly fine-tunes further differentiation and myelination of mature OL cells at later stages.

Considering that OL lineage cells and myelin-related genes and proteins are significantly decreased when iGluSnFR is expressed extracellularly under the GFAP promoter, we tested for diminished proliferation or increased apoptosis of OL lineage cells in iGluSnFR-expressing zfl brains and spinal cords. For this purpose, we assessed the expression of the proliferating cell nuclear antigen (Pcna) marker, a nuclear acidic protein required for DNA replication that is expressed through the cell cycle, to study the proliferative properties of

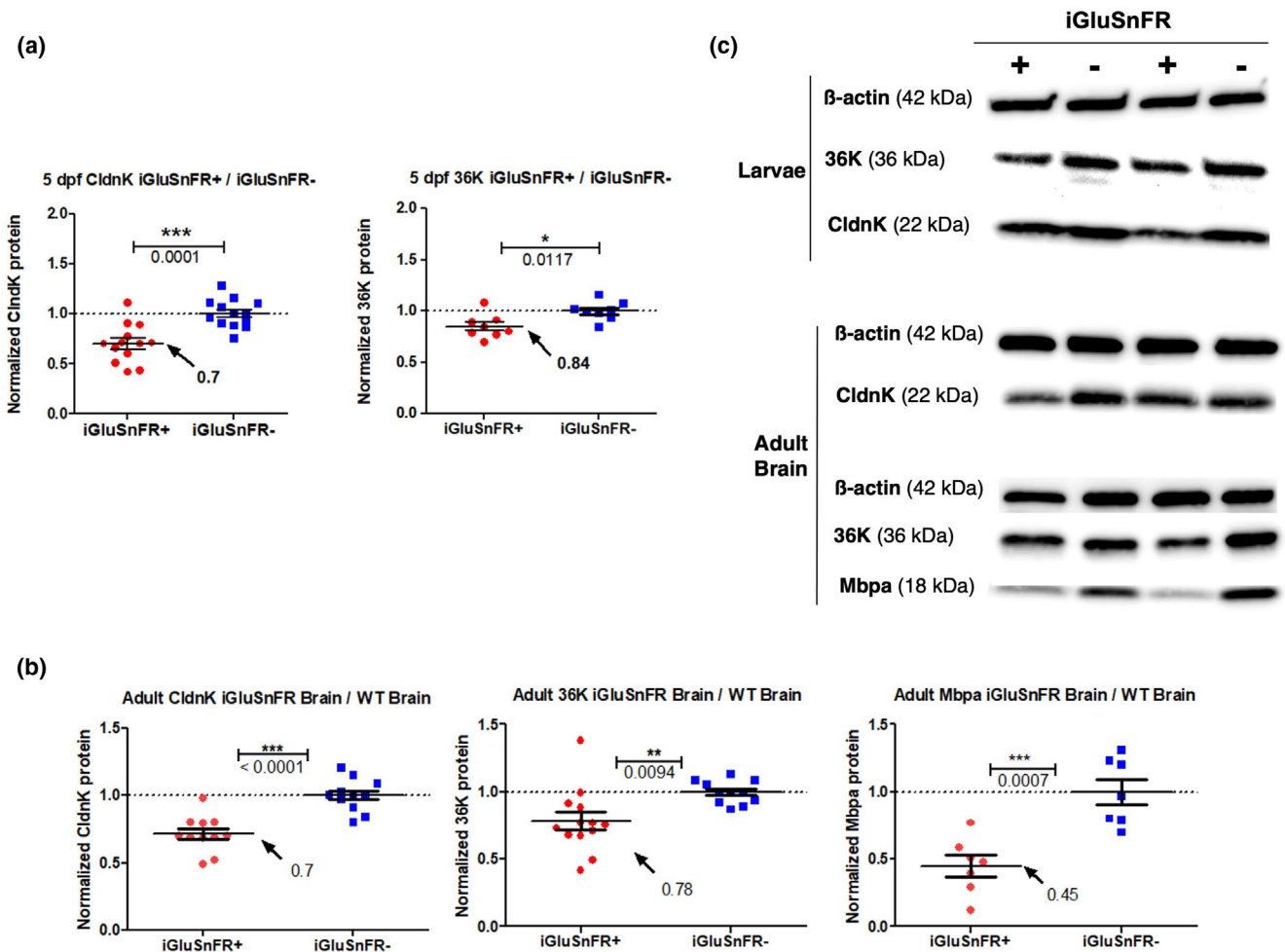


**FIGURE 5** Protein expression of myelin-related genes is significantly decreased in iGluSnFR-expressing 5 dpf zebrafish larvae and adult brains. (a) The expression of the myelin proteins CldnK (left) and 36K (right) is significantly decreased in iGluSnFR-expressing 5 dpf larvae (red), which is compared to iGluSnFR<sup>-</sup> littermate controls (blue). For both proteins, the ratio of iGluSnFR<sup>(+)</sup>/iGluSnFR<sup>(-)</sup> expression was calculated for each experiment and normalized against the average values of iGluSnFR<sup>(-)</sup> expression, which was thus set to one in average, as shown. Dot plot graphs are averaged (values shown in graphs) of pixel density areas of the according Western blot bands (mean  $\pm$  StDev). Data were analyzed by an unpaired two-tailed *t* test. *p*-Values are significant  $***p < 0.0001$ ;  $**p < 0.001$ ;  $*p < 0.05$ ; CldnK:  $p = 0.0001$ ;  $t = 4.500$ ; 36K:  $p = 0.0117$ ;  $t = 2.897$ ;  $N = 4$  independent experiments. (b) Normalized expression of the myelin proteins CldnK (left), 36K (middle), and Mbpa (right) are significantly decreased in iGluSnFR-expressing adult brains (red) compared to controls (WT brains; blue). As above for the zfl for all protein expression quantification, the ratio of iGluSnFR<sup>(+)</sup> brain/WT iGluSnFR<sup>(-)</sup> expression was calculated and normalized against the average values of iGluSnFR<sup>(-)</sup> expression (see methods section for details of calculations). Dot plot graphs show averaged values of pixel density areas of the according Western blot bands (mean  $\pm$  StDev). Data were analyzed by an unpaired two-tailed *t* test. CldnK:  $p < 0.0001$ ;  $t = 5.522$ ; 36K:  $p = 0.0094$ ;  $t = 2.848$ ; Mbpa:  $p = 0.0007$ ;  $t = 4.496$ .  $N = 3$  Independent experiments. (c) Representative Western blot protein expression bands of 36K, CldnK, Mbpa, and  $\beta$ -actin from 5 dpf zfl (upper panel) and adult brains (lower panel). For complete Western blot membranes, please refer to Figure S2 (zfl) and Figure S3 (adult brain)

oligodendrocyte lineage cells in iGluSnFR-expressing 5 dpf zfl brain and spinal cords compared to controls which do not express iGluSnFR. And indeed, the expression of iGluSnFR may impair the proliferation of OL lineage cells in our zf model. We found that the protein expression of PCNA (Figure S4c,d) was reduced in iGluSnFR-expressing zfl brain and spinal cord at 5 dpf together with Mbpa (Figure S4a,b), which was also true for PCNA in zf adult brain (Figure S5d). This finding puts forward our hypothesis and suggests that OL lineage cells proliferation failure correlates with the disruption of the myelination process in iGluSnFR-expressing zfl compared to controls.

In a second approach, cleaved caspase-3 (CC3) was used as a marker for apoptosis, to evaluate the activation of this process in brains and spinal cords of iGluSnFR-expressing zfl and adult brains compared to controls. Unlike Mbpa or PCNA, CC3 expression seems not to be changed in brains and spinal cords of iGluSnFR-expressing zfl nor in zf adult brains compared to controls (Figures S4e,f and S5e).

So far we have shown that glutamate signaling might be a crucial element for myelination regulation in the CNS. Though we only observed that OPCs, OL numbers as well as myelin-related gene and protein expression were significantly decreased in zf-expressing

iGluSnFR, which might have a sponge-like effect for extracellular glutamate. However, so far have not shown a direct link between OPCs, OL number, myelin-related gene expression, and glutamate, but only speculated about the glutamate-buffering effect of iGluSnFR.

Therefore, as a next step, we implemented an alternative pharmacological approach. In order to test our previous assumption, we used L-AP4 (L-2-amino-4-phosphonobutyric acid) that binds to the glutamate receptor and thereby increases its activity. L-AP4 is a commonly used drug that acts as a group-selective agonist for the group III metabotropic glutamate receptors (mGluRs). Thus, upon exposure to the L-AP4 agonist, mGluRs are being triggered and will enhance the underlying related cascades; along with this, it has been reported that L-AP4 mediates glutamatergic transmission through the activation of mGluR4 (Valenti et al., 2003).

We initially treated zfl with L-AP4 by bath immersion, using different increasing incubation concentrations of 25, 50, 100, and 250  $\mu$ M. We did not observe any clear effect of the L-AP4 bath treatment (data not shown). This might be because L-AP4 did not reach its target tissue. Therefore, to ensure that the developing CNS target is reached by L-AP4, we next decided to inject L-AP4 at a volume of approximately 6 nl and a concentration of 1mM into the brain ventricle of 3 dpf *Tg(CdnK:mem-TdTomato)* zfl. Our qRT-PCR results show that L-AP4 injected in this manner significantly increased the mRNA expression of the myelin-related genes *mbpa* and *plp1b* at 5 dpf (*mbpa*: L-AP4 versus Ctrl  $**p < 0.01$ ; L-AP4 versus uninj.  $**p < 0.01$ ; one-way ANOVA;  $F = 18.60$ ;  $df = 11$  and *plp1b*: L-AP4 versus Ctrl  $**p < 0.01$ ; L-AP4 versus uninj.  $**p < 0.01$ ; one-way ANOVA;  $F = 10.74$ ;  $df = 11$ ; Figure 6a), in comparison to both, uninjected and vehicle-treated zfl. L-AP4 injections did not affect the mRNA expression of housekeeping genes ( $\beta$ -actin: L-AP4 versus Ctrl  $p = 0.6673$ ; L-AP4 versus uninj.  $p = 0.6673$ ; one-way ANOVA;  $F = 0.4233$ ;  $df = 11$  and *ef1a*: L-AP4 versus Ctrl  $p = 0.8338$ ; L-AP4 versus uninj.  $p = 0.8338$ ; one-way ANOVA;  $F = 0.1855$ ;  $df = 11$ ).

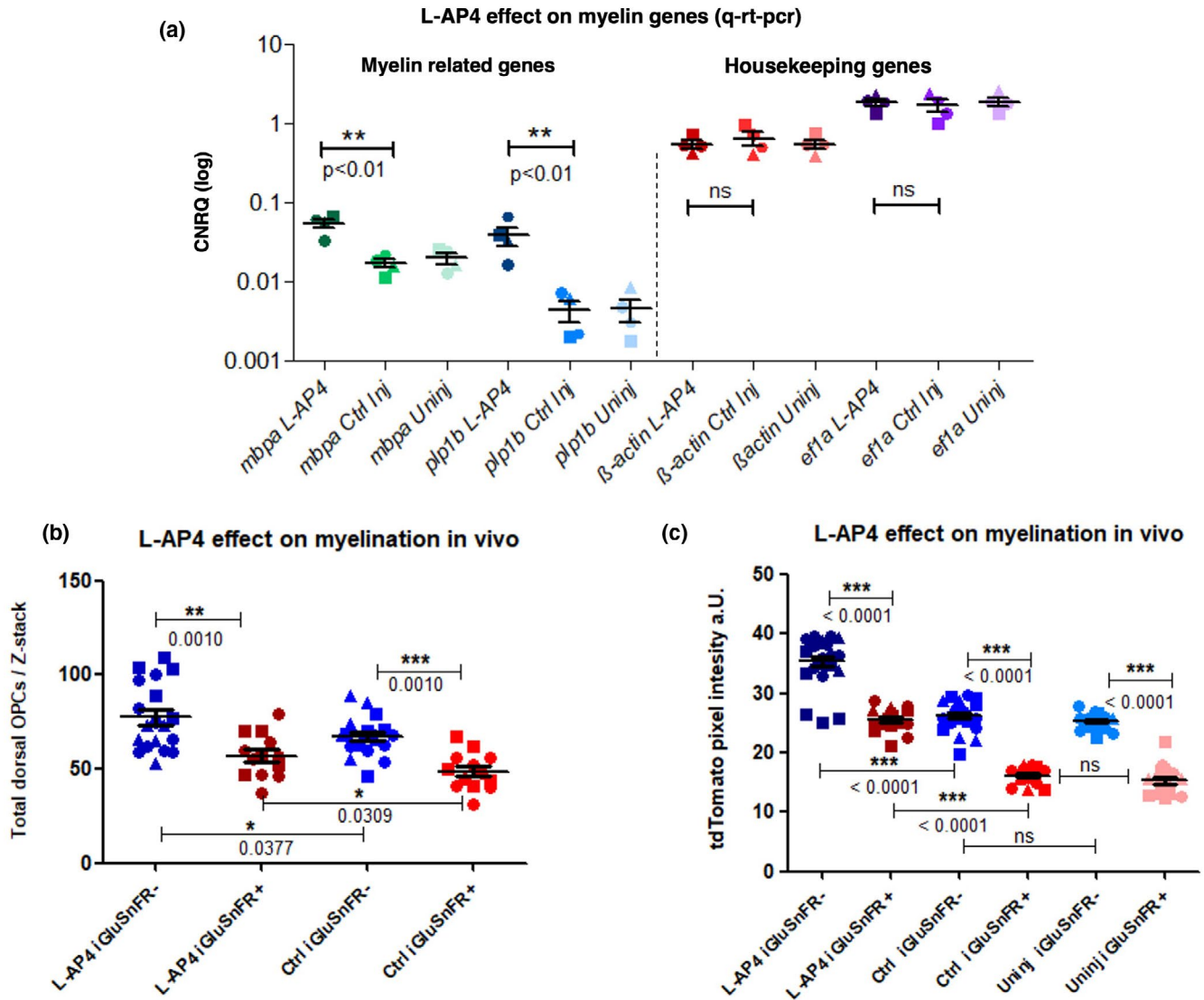
Further, these L-AP4 injection qRT-PCR results were confirmed as described before by dorsal OPC number calculation in *Tg(olig2:dsRed)* reporter-zfl (Figure 6b - compare to Figure 2c) and by spinal cord fluorescence intensity measurements in *Tg(cldnk:mem-TdTomato)* reporter-zfl (Figure 6c - compare to Figure 3d). In both cases, these experiments were performed in *Tg(GFAP:iGluSnFR)* positive<sup>(+)</sup> and/or negative<sup>(-)</sup> zfl. Total dorsal OPC numbers at 5 dpf were highest in L-AP4-treated iGluSnFR<sup>(-)</sup> *Tg(olig2:dsRed)* reporter-zfl. L-AP4 treatment of iGluSnFR<sup>(+)</sup> zfl partially but significantly ( $*p = 0.0309$ ; unpaired t test;  $t = 1.959$ ) rescued dorsal OPC numbers close to control-treated levels in iGluSnFR<sup>(-)</sup> zfl. As before at 3 dpf in iGluSnFR<sup>(+)</sup> also at 5 dpf dorsal OPC numbers were lowest in sham-injected iGluSnFR<sup>(+)</sup> zfl (Figure 6b). Low-resolution epifluorescence microscope image analysis of 5 dpf *Tg(CldnK:mem-TdTomato)*+ zfl shown in Figure 6c further confirm these results as well as the myelin-rescue effect of L-AP4 on iGluSnFR<sup>(+)</sup> zfl. The increase in the red fluorescent myelination reporter in L-AP4-injected zfl— injected at 3 dpf— compared to vehicle-treated and uninjected zfl was obvious at 5 dpf. As indicated in the corresponding graph, red

reporter-myelination was significantly increased in L-AP4-injected iGluSnFR<sup>(-)</sup> control zfl in comparison to the vehicle-treated and uninjected 5 dpf control zfl (LAP-4 versus Ctrl  $***p < 0.0001$ ;  $F = 82.24$ ;  $df = 69$ ; L-AP4 versus uninj.  $***p < 0.0001$ ;  $F = 82.24$ ;  $df = 69$  and Ctrl versus uninj nonsignificant;  $F = 82.24$ ;  $df = 69$ ; one-way ANOVA followed by Bonferroni's multiple comparisons). Compared to sham or nontreated iGluSnFR<sup>(+)</sup> zfl, the L-AP4-injected iGluSnFR<sup>(+)</sup> zfl were fully rescued to wt control myelin reporter fluorescent values. These data strongly suggest that the agonist/glutamate binding on its OPC and/or OL receptor, and the signaling cascade downstream, are involved in the myelination process and development within the CNS. Furthermore, the L-AP4 injection rescue experiments into the iGluSnFR<sup>(+)</sup> zfl further suggest the validity of our iGluSnFR glutamate-buffering hypothesis.

Opting for another pharmacological tool L-trans-pyrrolidine-2,4-dicarboxylate (PDC), which is a pharmacological agent known as a potent glutamate transport inhibitor (Matthews et al., 2003) and transporter substrate itself, we examined further if glutamate signaling is a critical factor for CNS myelination. We tested the effects of PDC (Sheldon & Robinson, 2007) on our zebrafish model, and thus further investigate the role of the glutamate machinery within the myelination process.

Additionally, we used the extinction of glutamate by enzymatic degradation as an alternative to glutamate receptor/transporter inhibition in impairing potential glutamate-dependent myelination. Glutamate pyruvate transaminase (GPT) is a remarkably effective glutamate-degrading enzyme, which requires pyruvate as a co-substrate though (Matthews et al., 2003). Therefore, we additionally investigated the use of GPT in combination with pyruvate to test for glutamate-dependent myelin regulation, as we propose it for the iGluSnFR<sup>(+)</sup> zfl. We injected different concentrations of either GPT + Pyruvate or PDC into the brain ventricle of 3 dpf *Tg(CldnK:mem-TdTomato)* zfl. Finally, we injected 10 U/ml GPT +50  $\mu$ M Pyruvate and independently 1mM PDC at a volume of ~6 nl into the brain ventricle of 3 dpf *Tg(CldnK:mem-TdTomato)* zfl. As shown in Figure 7a, the normalized mRNA expression of the myelin-related genes *mbpa* and *plp1b* was significantly decreased after treatment with GPT + Pyruvate or PDC by rt-PCR (*mbpa*: pdc versus ctrl  $*p < 0.05$ ;  $F = 13.51$ ;  $df = 11$ ; gpt versus ctrl  $**p < 0.01$ ;  $F = 13.51$ ;  $df = 11$  and for *plp1b*: pdc versus ctrl  $**p < 0.01$ ;  $F = 17.18$ ;  $df = 11$ ; gpt versus ctrl  $**p < 0.01$ ;  $F = 17.18$ ;  $df = 11$ ; one-way ANOVA followed by Bonferroni's multiple comparisons). This finding was further confirmed by in vivo imaging of the red myelin reporter fluorescence in 5 dpf *Tg(CldnK:mem-TdTomato)* zfl (Figure 7b). Our quantitative fluorescence data show that both GPT and PDC significantly diminish the myelination level based on the expression of the red fluorescent marker under the *CldnK* promoter in GPT- and PDC-treated zfl compared to control groups (gpt versus ctrl  $***p < 0.0001$ ;  $F = 27.48$ ;  $df = 104$  and pdc versus ctrl  $***p < 0.0001$ ;  $F = 27.48$ ;  $df = 104$ ; one-way ANOVA followed by Bonferroni's multiple comparisons; Figure 7c).

In summary, our results demonstrate that the availability of extracellular glutamate, and downstream signaling related to



glutamate, plays a crucial role within the regulation of the CNS myelination process.

## 4 | DISCUSSION

Throughout the brain and spinal cord, specialized mechanisms for myelin regulation are required to maintain the physiology and connectivity of neurons. Recently, the regulation and variation of CNS myelination has been discussed as a possible source of “neuronal” computational plasticity (Almeida & Lyons, 2017; Dutta et al., 2018). The axon and its enwrapping myelin sheath form a functional unit that enables a fast and timely exchange of information in the CNS. In this context, a diverse set of mechanisms have been implicated in the control of oligodendroglia differentiation and myelination. Importantly myelination can be induced by action potential firing in axons (Fields, 2015; Wake et al., 2011). The large majority of myelinated projection neurons are glutamatergic. OPCs collect glutamatergic synaptic inputs coming from un-myelinated axons (Barron

& Kim, 2019; Berret et al., 2017; Kukley et al., 2007; Micu et al., 2016) and OL lineage cells express glutamate receptors, which allow them to respond to alteration in neuronal activity (Almeida et al., 2020; Barron & Kim, 2019; Berret et al., 2017). Although there is a large body of literature on glial glutamate signaling (Barron & Kim, 2019; Berret et al., 2017), the role of this signaling in myelination is still not entirely clear. In the present report, we studied the glutamate-related mechanisms implicated in myelin regulation and provide new evidence and data on glutamate signaling as a potential modulator of initial CNS myelination. Although altered extracellular glutamate also potentially affects earlier neurogenesis and gliogenesis, we do not think this is the case here in our study as the iGluSnFR reporter is only expressed under the activation of the GFAP promoter. Therefore at the time point of iGluSnFR expression and our pharmacological treatments, these two developmental (time) phases, initial neurogenesis and gliogenesis, should be passed and therefore not be effected. But still, we cannot completely rule out that there is some direct glutamate effect on proliferating and developing neurons and their axons as well, as we did not test for this in our present

**FIGURE 6** Treatment with the mGluR agonist L-AP4 increased myelin-related genes and rescues CNS myelination in iGluSnFR<sup>(+)</sup> zfl. (a) CNRQ values representing mRNA quantification of *mbpa*, *plp1b*,  $\beta$ -actin, and *ef1a* isolated from 1mM L-AP4, sham vehicle-injected and untreated zfl (wild type) at 5 dpf (injected at 3 dpf). mRNA levels were normalized against  $\beta$ -actin and *ef1a* housekeeping gene expression. Both myelin genes, *mbpa* and *plp1b*, show a significant increase in expression in L-AP4 injected zfl compared to sham-injected or uninjected control larvae. Both housekeeping genes though do not show any significant difference in L-AP4 versus sham-injected or uninjected controls. Data were evaluated by one-way ANOVA followed by Bonferroni's multiple comparisons. \* indicates a  $p$ -value < 0.05; \*\* indicates a  $p$ -value < 0.01. Values show mean  $\pm$  SEM. *mbpa*: L-AP4 versus Ctrl \*\* $p$  < 0.01; L-AP4 versus uninj. \*\* $p$  < 0.01;  $F = 18.60$ ;  $df = 11$  and *plp1b*: L-AP4 versus Ctrl \*\* $p$  < 0.01; L-AP4 versus uninj. \*\* $p$  < 0.01;  $F = 10.74$ ;  $df = 11$ ;  $\beta$ -actin: L-AP4 versus Ctrl  $p = 0.6673$ ; L-AP4 versus uninj.:  $p = 0.6673$ ;  $F = 0.4233$ ;  $df = 11$  and *ef1a*: L-AP4 versus Ctrl  $p = 0.8338$ ; L-AP4 versus uninj.  $p = 0.8338$ ;  $F = 0.1855$ ;  $df = 11$ .  $N = 4$  independent experiments indicated by different shapes. (b) Two-photon in vivo microscopic images of *Tg(Olig2:dsRed)* proximal zfl spinal cords of 5 dpf larvae after L-AP4 ventricle injections at 3 dpf where analyzed in lateral view. For representative example images, please refer to Figure S6a. A significant increase in total dorsal OPCs after L-AP4 injection could be seen in iGluSnFR<sup>(-)</sup> zfl compared to sham-injected iGluSnFR<sup>(-)</sup> larvae. \* $p = 0.0377$ ; unpaired two-tailed  $t$  test;  $t = 2.158$ . iGluSnFR<sup>(+)</sup> zfl at 5 dpf like before at 3 dpf (see Figure 2) showed a significant \*\*\* $p = 0.001$ ; unpaired two-tailed  $t$  test;  $t = 3.643$  decrease in dorsal OPCs compared to iGluSnFR<sup>(-)</sup> zfl. Injection of 1mM L-AP4 at 3 dpf into the ventricle of iGluSnFR<sup>(+)</sup> zfl though could partly but significantly \* $p = 0.0309$ ; unpaired  $t$  test;  $t = 1.959$  rescue the OPC reducing effect of iGluSnFR at 5 dpf. Dot plot graphs show averages of dorsal OPC numbers (mean  $\pm$  StDev).  $N = 3$  independent experiments indicated by different shaped dots, with a total ( $n$ ) of 13–19 larvae. (c) Low-resolution epi-fluorescence microscopic images of *Tg(CaudinK:mem-TdTomato)* proximal zfl spinal cords of 5 dpf larvae after L-AP4 or sham ventricle injections at 3 dpf where analyzed in lateral view. For representative example images, please refer to Figure S6b. A significant increase in tdTomato red myelin reporter fluorescence after L-AP4 injection could be seen in iGluSnFR<sup>(-)</sup> zfl compared to sham-injected iGluSnFR<sup>(-)</sup> larvae \*\*\* $p < 0.0001$ ; one-way ANOVA followed by Bonferroni's multiple comparisons;  $F = 82.24$ ;  $df = 69$ . The same is true for a comparison with completely uninjected iGluSnFR<sup>(-)</sup> siblings. Control iGluSnFR<sup>(+)</sup> zfl at 5 dpf like before (see Figure 3c) showed a significant \*\*\* $p < 0.0001$ ; unpaired two-tailed  $t$  test;  $t = 9.378$ ; decrease in tdTomato reporter fluorescence compared to control iGluSnFR<sup>(-)</sup> zfl. Injection of 1mM L-AP4 at 3 dpf into the ventricle of iGluSnFR<sup>(+)</sup> zfl though could completely and significantly \*\*\* $p < 0.0001$ ; rescue this myelin-reducing effect of iGluSnFR at 5 dpf; one-way ANOVA followed by Bonferroni's multiple comparisons;  $F = 172.2$ ;  $df = 54$ . Dot plot graphs show averages of red tdTomato myelin reporter fluorescence (mean  $\pm$  StDev).  $N = 3$  independent experiments indicated by different shaped dots, with a total ( $n$ ) of 15–17 larvae

experiments here. A potential direct glutamate effect on neurons again could cause and explain for some changes on OPCs, OLs, and myelination for sure.

One of our major findings in the zebrafish model is that signaling mechanisms regulating myelination are dependent on the extracellular glutamate concentration. In support of this finding are a number of reports showing that myelination can be controlled by regulating vesicular release from neurons reporting from cell culture (Wake et al., 2011, 2015), mouse (Evonuk et al., 2020; Kougioumtzidou et al., 2017), and other zebrafish models (Hines et al., 2015; Koudelka et al., 2016; Mensch et al., 2015). In the latter report, the authors evaluated myelin sheet dynamics along single axons over time using live imaging approaches within the zf model and proposed a general role for vesicular—possibly glutamate—release in the elongation of maturing myelin sheets. Our study using a genetically engineered fluorescent protein sensitive to glutamate (iGluSnFR) now demonstrates that the diminution of OPCs as well as mature OLs is evidently associated with the expression of this glutamate reporter and the reduction of extracellular glutamate in the CNS. This decrease in OPCs and OLs was not seen when a GFAP-GFP fusion protein was expressed under the very same GFAP promoter (see controls in Figures 1 and 2). Therefore, we can rule out that this OL and myelination decrease is somehow caused by the promoter or a sheer overexpression of a fluorescent protein. Furthermore, the decrease in OPCs, OLs, and myelination in iGluSnFR<sup>(+)</sup> zfl could be significantly rescued by the injection of the glutamate agonist L-AP4 (Figure 6b,c), which supports our idea of iGluSnFR as a glutamate sink or sponge in the here used *Tg(GFAP:iGluSnFR)* fish model.

With respect to neuron to glia signaling, we show in our GPT and PDC injection experiments that glutamate transport and extracellular glutamate concentrations are functionally relevant (Figure 7). And our observations suggest in the same way that if glutamate is being bound or being buffered away by iGluSnFR, it becomes conceivably less available in the extracellular space, and thus glutamate exerts less of its physiological function through its corresponding ionotropic and metabotropic receptors, behind which again complex multifaceted cascades are triggered. Alongside with this, in cultured OPCs it has been shown, that activation of group 1 mGluRs (presumably mGluR5) enhances the intracellular calcium (Luyt et al., 2003), which again causes the release of brain-delivered neurotrophic factor (BDNF) (Bagayogo & Dreyfus, 2009). BDNF again may either promote myelin formation and/or reduce both excitotoxic damage to the cells as well as apoptosis (Deng et al., 2004; Kelland & Toms, 2001; Luyt et al., 2006). This led us to believe again that the observed decrease in myelination, shown by the decrease of myelin-related genes in this study, is likely associated with a decrease in glutamate-induced mGluR activation in the presence of iGluSnFR, as iGluSnFR binds specifically to glutamate and so making it less available in the extracellular space.

Our data are consistent with the fact that glutamate is essential for excitatory synaptic transmission (Xin et al., 2019) and thus an important player within the activity-driven adaptive myelination concept (Almeida et al., 2020; Baraban et al., 2016). Recent reports using different in vivo preparations have further shown that either neuronal activity (Almeida et al., 2020; Ortiz et al., 2019) or the abrogation of vesicular release (Ettxeberria et al., 2016; Mensch et al., 2015) alters the myelination of neuronal fibers in different

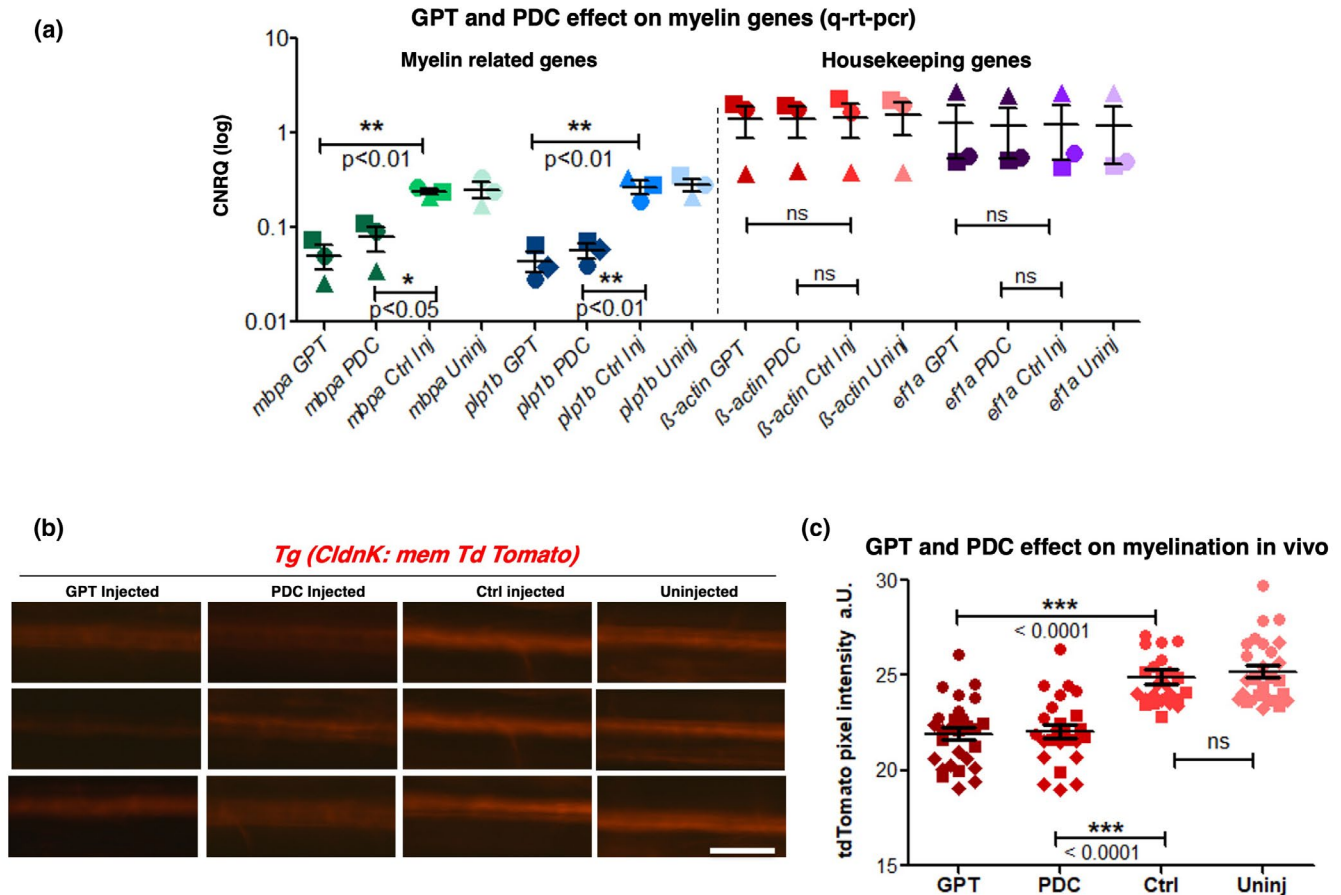


**FIGURE 7** Glutamate degrading and blockade of glutamate uptake significantly decreased myelin-related genes and myelination. (a) After zfl ventricle injections at 3 dpf with the Glutamate-Pyruvate-Transaminase (GPT) and the glutamate transport inhibitor L-trans-pyrrolidine-2,4-dicarboxylate (PDC), CNRQ values representing mRNA quantification of *mbpa*, *plp1b*,  $\beta$ -actin, and *ef1a* genes were analyzed. Data are from 10 U/ml GPT + 50  $\mu$ M Pyruvate, 2 mM PDC, sham vehicle-injected and untreated zebrafish larvae (wild type, 5 dpf). The housekeeping genes  $\beta$ -actin and *ef1a* do not show any significant difference. mRNA levels could therefore be normalized against  $\beta$ -actin and *ef1a* housekeeping gene expression. For both pharmacological treatments supposed to reduce extracellular glutamate, we could find a significant decrease of the myelin-related genes *mbpa* and *plp1b* in 5 dpf zfl. Data were evaluated by one-way ANOVA followed by Bonferroni's multiple comparisons to compare the means among the four groups. \*\* indicates a  $p$ -value < 0.01; \*\*\* indicates a  $p$ -value < 0.001. Values show mean  $\pm$  SEM.  $N = 3$  independent experiments indicated by different shaped dots. (b) Low-resolution epi-fluorescence microscopic images of 5 dpf Tg(CldnK:mem-TdTomato) zfl spinal cords in lateral view demonstrate in vivo decrease of myelination after injections of GPT and PDC at 3 dpf. Clear decrease in myelination in 10 U/ml GPT + 50  $\mu$ M Pyruvate-treated larvae (left column) and 2 mM PDC-treated larvae (second from left) could be seen compared to sham vehicle-injected (second from right) or uninjected larvae (right) controls by examination of ClaudinK:mem-TdTomato fluorescence intensities as direct myelin reporter. Scale bar 50  $\mu$ m. (c) Quantification of relative CldnK:mem-TdTomato fluorescence intensities as a parameter for myelination. Images of all experiment were acquired under the same microscopy settings. The fluorescence level (pixel intensity) of the proximal spinal cord of each fish was quantified at the same selected region. Both 10 U/ml GPT + 50  $\mu$ M Pyruvate and 2 mM PDC injected larvae show a significant decrease in myelination compared to the sham vehicle-injected control or the uninjected control. While no difference is seen between uninjected versus vehicle-injected larvae. Dot plot graphs show average values of pixel density areas as mean  $\pm$  StDev.  $p$ -values are significant \*\*\* $p$  < 0.001; one-way ANOVA followed by Bonferroni's multiple comparisons.  $N = 3$  independent experiments with a total of 90 to 110 larvae ( $n$ ). Each dot shape indicates the identity of a certain data point to the appropriate experiment ( $N$ )

ways. Furthermore, overstimulation of ionotropic glutamate receptors is a pathological process causing excessive calcium influx that induces excitotoxicity to neurons, which is a pivotal mechanism implicated in neurodegenerative diseases as demonstrated by Evonuk et al. (2020) and Xin et al. (2019). Oligodendrocytes also express ionotropic glutamate receptors, which are sensitive to excitotoxicity. It has recently been shown that genetic deletion of specific glutamate receptors/subunits such as AMPAR/gluA4 in oligodendrocytes

in mice alleviated an induced loss of myelinated axons (Evonuk et al., 2020). In this study, the authors show that glutamate-induced calcium influx through AMPAR into mature oligodendrocytes facilitate excitotoxic damage to their myelin sheet and consequently causes a loss of axons in a mouse model of autoimmune inflammatory demyelination (Evonuk et al., 2020), while other studies propose a myelin-independent role for glutamate signaling in this context (Xin et al., 2019).

It is well-described that CNS remyelination can be actively processed by already existing OPCs, that then migrate to the site of injury, proliferate, differentiate, and wrap their processes around the demyelinated axons to form a new myelin sheath (Chamberlain et al., 2016; Tognatta & Miller, 2016). In agreement with this assumption, elegant studies in an ethidium bromide lesion model in rats (Gautier et al., 2015) and in an alysolecithin lesion model in mice together with MS patient studies (Etxeberria et al., 2010; Sahel et al., 2015) showed that partially damaged demyelinated axons (mentioned above) upregulate presynaptic proteins to form synapses with recruited (migrated) OPCs. Of importance, these OPCs express AMPA/kainate and also NMDA glutamate receptors (Li et al., 2013; Lundgaard et al., 2013), which might explain three things: first, the implication of glutamate in this process, whose receptors are located on OPCs, and second the important role of oligodendrocyte lineage cell proliferation and differentiation in remyelination and third the interplay between these two facts. Along with this, Barron and Kim (2019) describe the functional link between glutamatergic input and calcium entry in OLs. They demonstrate a mechanism how glutamate causes an increase in calcium signaling in OLs within the auditory brainstem. In our study, we now found further supporting evidence in this context as: first OPC and OL numbers and second pixel intensity related to their fluorescent myelin markers Olig2 (for OPCs) and CldnK (for OLs) both decrease either in iGluSnFR-expressing zfl (Figures 1–3) or in pharmacological-treated zfl (Figure 7) by which extracellular glutamate is reduced in the CNS. This indicates that either proliferation is decreased or apoptosis is increased causing a decrease in OPC and OL numbers and related fluorescence pixel intensity. To ascertain this proliferation and/or apoptosis hypothesis, we studied cell proliferation using PCNA as a marker and could find a considerable decrease in PCNA expression in the brains and spinal cords of iGluSnFR-expressing zfl as well as in adult zf brains (Figures S3d and S4c,d). In connection with this, myelin-related proteins such as Mbpa, CldnK, and 36K were less expressed in the brains and spinal cords of zfl and adult zf brains expressing iGluSnFR compared to controls (Figure S4a,b and S5a–c). This finding further supports that glutamate signaling is required for OPC proliferation.

However, apoptotic pathways do not seem to be implicated in the reduction of OL lineage cells within the iGluSnFR<sup>(+)</sup>  fish, as suggested by Figures S4e,f and S5e, showing no difference of expression in the apoptosis marker CC3 in iGluSnFR-expressing fish compared to controls. Taken together, glutamate can therefore be implicated in the control of proliferation of OL lineage cells, known to receive glutamatergic receptor-mediated synaptic input from neurons (Chen et al., 2018). This finding further emphasizes the concept that glutamate released at neuron–glia synapses does convey the consequences of neuronal activity on proliferation of OL lineage cells as suggested by Mount and Monje (2017) and supported by our proliferation data. Other studies putting forward this hypothesis indicate that some forms of neuronal activity facilitate proliferation (Chen et al., 2018; Mount & Monje, 2017), while others boost differentiation (Chen et al., 2018; Nagy et al., 2017). In this context, similar to

our study where we manipulate glutamate signaling using iGluSnFR as a genetic tool, in 2017 Kougioumtzidou et al., showed that genetic disruption of glutamatergic receptors in OPCs promoted apoptotic death of oligodendrocytes, which indicated that axon–OPC synapses are considered as critical for the structural and functional communication between the two cell types (Kukley et al., 2007; Kula et al., 2019), even though we could not see any obvious apoptotic effect in our study in the fish now.

We observed a significant decrease in expression of myelin-related genes when extracellular glutamate was potentially buffered away by the iGluSnFR and/or after pharmacological manipulation with a potential similar effect in our zf model. These results support further that glutamate is essential for proper myelination, but is seemingly contradicting the glutamate-induced excitotoxicity hypothesis (Pitt et al., 2000). Nevertheless, we still think that glutamate may provoke excitotoxic cell death mediated by an “overactivation” of glutamate receptors, which is then associated with an extensive calcium influx toxic to the cells and to sodium influx resulting in swelling and lysis of cells, which again may in turn induce a release of even more glutamate (Káradóttir & Attwell, 2007; Trump & Berezsky, 1996). But, in parallel, it has been demonstrated that myelination, as well as remyelination, is regulated by neuronal activity and tightly associated with glutamate release from, for example, the demyelinated axon (Gautier et al., 2015; Lundgaard et al., 2013). Therefore these studies—in agreement with ours—strongly suggest that although being toxic at high unnatural concentrations, extracellular glutamate levels at “normal” concentrations do have a directive and necessary regulative impact on myelination and therefore blocking or lowering glutamate uptake or the glutamate pool does negatively influence OL development and thus dysregulates the myelination process.

In agreement with this concept, using two specific pharmacological agents, GPT, which is degrading glutamate (Matthews et al., 2003) and PDC, which is blocking glutamate reuptake (Matthews et al., 2000), in our present study, we demonstrate that glutamate promotes myelination. Our data further show that the exogenous glutamate agonist L-AP4 considerably increased the expression of myelin-related genes, *mbpa* and *plp1b*, in zfl. This suggests that glutamate-binding and/or the signaling cascade downstream of glutamate plays a pivotal role in the myelination process, which certainly needs to be further investigated. It seems that machineries related to glutamate receptors are complex and it is conceivable that metabotropic glutamate receptors, AMPA/kainate and NMDA receptors serve various different functions in regulating differentiation and myelination, as well as in the later homeostasis of OLs in general.

The L-AP4 injection (rescue) data also support our concept that the physiological glutamate level was decreased in the presence of iGluSnFR, which initially was intended to visualize glutamate release by neurons and astrocytes (Marvin et al., 2013). But it needs to be considered now, that, this unwanted glutamate decrease caused by the iGluSnFR expression impacts negatively on the myelination process, as we observed a drastic reduction of myelin markers when

iGluSnFR was expressed. This fact needs to be seen and discussed as an undesirable side effect of this fluorescent glutamate reporter. Further, one needs to consider this unwanted potential buffering effect on a signaling molecule seen in our study for iGluSnFR possibly for other in vivo reporters (Ni et al., 2018) like, for example, GCaMPs or similar as well.

Taken together, our zf study provides new evidence on how, when, and where glutamate may impact on the CNS myelination process and suggests different pharmacologically controllable gates, by which glutamate signaling in related diseases could potentially be therapeutically modulated.

## DECLARATION OF TRANSPARENCY

The authors, reviewers and editors affirm that in accordance to the policies set by the *Journal of Neuroscience Research*, this manuscript presents an accurate and transparent account of the study being reported and that all critical details describing the methods and results are present.

## ACKNOWLEDGMENTS

The authors are grateful for a NRW-Repatriation grant and the German Research Foundation (DFG) equipment grant (INST 1172/37-1 FUGG) for a multi-photon microscope setup to B.O. They thank Professor D. Lyons and Professor C. G. Becker, Edinburgh and the European Zebrafish Resource Centre (EZRC), Karlsruhe for transgenic fish lines. They are also thankful to the Zebrafish Core Facility (Bonn Medical Faculty). They thank Dr. Henning Kleinert for initiation of the zebrafish rt-PCR protocols, Professors K. Schilling, S. Baader, and all members of the Odermatt Lab for their support and helpful discussions. They thank Professor Dr. Uwe Strähle, from KIT-Institute for Toxicology und Genetics (ITG) Karlsruhe for providing them with the *Tg(GFAP:GFAP-GFP)* zf line.

## CONFLICT OF INTEREST

The authors declare no conflict of interest.

## AUTHOR CONTRIBUTIONS

*Conceptualization*, F.T., C.L., L.S., A.H., and B.O.; *Methodology*, F.T., C.L., L.S., A.H., and B.O.; *Visualization*, F.T.; *Formal Analysis*, F.T., L.S., D.W., T.D., and B.O.; *Investigation*, F.T., C.L., L.S., S.A., T.L., J.C.K., A.H., and Ö.Y.; *Resources*, R.B.M.; *Writing – Original Draft*, F.T. and B.O.; *Writing – Review & Editing*, F.T. and B.O.; *Supervision*, B.O.; *Funding Acquisition*, B.O.

## PEER REVIEW

The peer review history for this article is available at <https://publons.com/publon/10.1002/jnr.24940>.

## DATA AVAILABILITY STATEMENT

The data that support the findings of this study are available from the corresponding author upon reasonable request.

## ORCID

Benjamin Odermatt  <https://orcid.org/0000-0002-9361-2772>

## REFERENCES

- Almeida, R. G., & Lyons, D. A. (2017). On myelinated axon plasticity and neuronal circuit formation and function. *Journal of Neuroscience*, *37*(42), 10023–10034. <https://doi.org/10.1523/JNEUROSCI.3185-16.2017>
- Almeida, R. G., Williamson, J. M., Madden, M. E., Early, J. J., Voas, M. G., Talbot, W. S., Bianco, I. H., & Lyons, D. A. (2020). Synaptic vesicle fusion along axons is driven by myelination and subsequently accelerates sheath growth in an activity-regulated manner. *BioRxiv*. <https://doi.org/10.1101/2020.08.28.271593>
- Bagayogo, I. P., & Dreyfus, C. F. (2009). Regulated release of BDNF by cortical oligodendrocytes is mediated through metabotropic glutamate receptors and the PLC pathway. *ASN Neuro*, *1*(1), AN20090006. <https://doi.org/10.1042/AN20090006>
- Baraban, M., Mensch, S., & Lyons, D. A. (2016). Adaptive myelination from fish to man. *Brain Research*, *1641*, 149–161. <https://doi.org/10.1016/j.brainres.2015.10.026>
- Barron, T., & Kim, J. H. (2019). Neuronal input triggers  $Ca^{2+}$  influx through AMPA receptors and voltage-gated  $Ca^{2+}$  channels in oligodendrocytes. *Glia*, *67*(10), 1922–1932. <https://doi.org/10.1002/glia.23670>
- Baumann, N., & Pham-Dinh, D. (2001). Biology of oligodendrocyte and myelin in the mammalian central nervous system. *Physiological Reviews*, *81*(2), 871–927. <https://doi.org/10.1152/physrev.2001.81.2.871>
- Bergles, D. E., Jabs, R., & Steinhäuser, C. (2010). Neuron-glia synapses in the brain. *Brain Research Reviews*, *63*(1–2), 130–137. <https://doi.org/10.1016/j.brainresrev.2009.12.003>
- Berret, E., Barron, T., Xu, J., Debner, E., Kim, E. J., & Kim, J. H. (2017). Oligodendroglial excitability mediated by glutamatergic inputs and Nav1.2 activation. *Nature Communications*, *8*(557). <https://doi.org/10.1038/s41467-017-00688-0>
- Chamberlain, K. A., Nanesco, S. E., Psachoulia, K., & Huang, J. K. (2016). Oligodendrocyte regeneration: Its significance in myelin replacement and neuroprotection in multiple sclerosis. *Neuropharmacology*, *110*, 633–643. <https://doi.org/10.1016/j.neuropharm.2015.10.010>
- Chen, S. L., März, M., & Strähle, U. (2009). gfap and nestin reporter lines reveal characteristics of neural progenitors in the adult zebrafish brain. *Developmental Dynamics*, *238*(2), 475–486. <https://doi.org/10.1002/dvdy.21853>
- Chen, T. J., & Kukley, M. (2020). Glutamate receptors and glutamatergic signalling in the peripheral nerves. *Neural Regeneration Research*, *15*(3), 438. <https://doi.org/10.4103/1673-5374.266047>
- Chen, T. J., Kula, B., Nagy, B., Barzan, R., Gall, A., Ehrlich, I., & Kukley, M. (2018). In vivo regulation of oligodendrocyte precursor cell proliferation and differentiation by the AMPA-receptor subunit GluA2. *Cell Reports*, *25*(4), 852–861. <https://doi.org/10.1016/j.celrep.2018.09.066>
- De Biase, L. M., Nishiyama, A., & Bergles, D. E. (2010). Excitability and synaptic communication within the oligodendrocyte lineage. *Journal of Neuroscience*, *30*(10), 3600–3611. <https://doi.org/10.1523/JNEUROSCI.6000-09.2010>
- Deng, W., Wang, H., Rosenberg, P. A., Volpe, J. J., & Jensen, F. E. (2004). Role of metabotropic glutamate receptors in oligodendrocyte excitotoxicity and oxidative stress. *Proceedings of the National Academy of Sciences of the United States of America*, *101*(20), 7751–7756. <https://doi.org/10.1073/pnas.0307850101>
- Dutta, D. J., Woo, D. H., Lee, P. R., Pajevic, S., Bukalo, O., Huffman, W. C., Wake, H., Basser, P. J., SheikhBahaei, S., Lazarevic, V., Smith, J. C., & Fields, R. D. (2018). Regulation of myelin structure and conduction velocity by perinodal astrocytes. *Proceedings of the National Academy of Sciences of the United States of America*, *115*(46), 11832–11837. <https://doi.org/10.1073/pnas.1811013115>



- Etcheberria, A., Hokanson, K. C., Dao, D. Q., Mayoral, S. R., Mei, F., Redmond, S. A., Ullian, E. M., & Chan, J. R. (2016). Dynamic modulation of myelination in response to visual stimuli alters optic nerve conduction velocity. *Journal of Neuroscience*, *36*(26), 6937–6948. <https://doi.org/10.1523/JNEUROSCI.0908-16.2016>
- Etcheberria, A., Mangin, J. M., Aguirre, A., & Gallo, V. (2010). Adult-born SVZ progenitors receive transient synapses during remyelination in corpus callosum. *Nature Neuroscience*, *13*(3), 287–289. <https://doi.org/10.1038/nn.2500>
- Evonuk, K. S., Doyle, R. E., Moseley, C. E., Thornell, I. M., Adler, K., Bingaman, A. M., Bevenssee, M. O., Weaver, C. T., Min, B., & DeSilva, T. M. (2020). Reduction of AMPA receptor activity on mature oligodendrocytes attenuates loss of myelinated axons in autoimmune neuroinflammation. *Science Advances*, *6*(2), eaax5936. <https://doi.org/10.1126/sciadv.aax5936>
- Fields, R. D. (2015). A new mechanism of nervous system plasticity: Activity-dependent myelination. *Nature Reviews Neuroscience*, *16*(12), 756–767. <https://doi.org/10.1038/nrn4023>
- Gautier, H. O. B., Evans, K. A., Volbracht, K., James, R., Sitnikov, S., Lundgaard, I., James, F., Lao-Peregrin, C., Reynolds, R., Franklin, R. J. M., & Káradóttir, R. T. (2015). Neuronal activity regulates remyelination via glutamate signalling to oligodendrocyte progenitors. *Nature Communications*, *6*(8518). <https://doi.org/10.1038/ncomms9518>
- Gupta, T., & Mullins, M. C. (2010). Dissection of organs from the adult zebrafish. *Journal of Visualized Experiments*, *37*(e1717). <https://doi.org/10.3791/1717>
- Gutzman, J. H., & Sive, H. (2009). Zebrafish brain ventricle injection. *Journal of Visualized Experiments*, *26*(e1218). <https://doi.org/10.3791/1218>
- Hellemsans, J., Mortier, G., De Paepe, A., Speleman, F., & Vandesompele, J. (2008). qBase relative quantification framework and software for management and automated analysis of real-time quantitative PCR data. *Genome Biology*, *8*(R19). <https://doi.org/10.1186/gb-2007-8-2-r19>
- Hines, J. H., Ravanelli, A. M., Schwindt, R., Scott, E. K., & Appel, B. (2015). Neuronal activity biases axon selection for myelination in vivo. *Nature Neuroscience*, *18*(5), 683–689. <https://doi.org/10.1038/nn.3992>
- Jantzie, L. L., Talos, D. M., Selip, D. B., An, L., Jackson, M. C., Folkert, R. D., Deng, W., & Jensen, F. E. (2010). Developmental regulation of group I metabotropic glutamate receptors in the premature brain and their protective role in a rodent model of periventricular leukomalacia. *Neuron Glia Biology*, *6*(4), 277–288. <https://doi.org/10.1017/S1740925X11000111>
- Káradóttir, R., & Attwell, D. (2007). Neurotransmitter receptors in the life and death of oligodendrocytes. *Neuroscience*, *145*(4), 1426–1438. <https://doi.org/10.1016/j.neuroscience.2006.08.070>
- Kelland, E. E., & Toms, N. J. (2001). Group I metabotropic glutamate receptors limit AMPA receptor-mediated oligodendrocyte progenitor cell death. *European Journal of Pharmacology*, *424*(3), R3–R4. [https://doi.org/10.1016/S0014-2999\(01\)01157-8](https://doi.org/10.1016/S0014-2999(01)01157-8)
- Kimmel, C. B., Ballard, W. W., Kimmel, S. R., Ullmann, B., & Schilling, T. F. (1995). Stages of embryonic development of the zebrafish. *Developmental Dynamics*, *203*(3), 253–310. <https://doi.org/10.1002/aja.1002030302>
- Kirby, B. B., Takada, N., Latimer, A. J., Shin, J., Carney, T. J., Kelsh, R. N., & Appel, B. (2006). In vivo time-lapse imaging shows dynamic oligodendrocyte progenitor behavior during zebrafish development. *Nature Neuroscience*, *9*(12), 1506–1511. <https://doi.org/10.1038/nn1803>
- Kolodziejczyk, K., Saab, A. S., Nave, K. A., & Attwell, D. (2010). Why do oligodendrocyte lineage cells express glutamate receptors? *F1000 Biology Reports*, *2*(57). <https://doi.org/10.3410/B2-57>
- Koudelka, S., Voas, M. G. G., Almeida, R. G. G., Baraban, M., Soetaert, J., Meyer, M. P. P., Talbot, W. S. S., & Lyons, D. A. A. (2016). Individual neuronal subtypes exhibit diversity in CNS myelination mediated by synaptic vesicle release. *Current Biology*, *26*(11), 1447–1455. <https://doi.org/10.1016/j.cub.2016.03.070>
- Kougioumtzidou, E., Shimizu, T., Hamilton, N. B., Tohyama, K., Sprengel, R., Monyer, H., Attwell, D., & Richardson, W. D. (2017). Signalling through AMPA receptors on oligodendrocyte precursors promotes myelination by enhancing oligodendrocyte survival. *eLife*, *6*(e28080). <https://doi.org/10.7554/eLife.28080>
- Kucenas, S., Takada, N., Park, H. C., Woodruff, E., Broadie, K., & Appel, B. (2008). CNS-derived glia ensheath peripheral nerves and mediate motor root development. *Nature Neuroscience*, *11*(2), 143–151. <https://doi.org/10.1038/nn2025>
- Kukley, M., Capetillo-Zarate, E., & Dietrich, D. (2007). Vesicular glutamate release from axons in white matter. *Nature Neuroscience*, *10*(3), 311–320. <https://doi.org/10.1038/nn1850>
- Kula, B., Chen, T. J., & Kukley, M. (2019). Glutamatergic signaling between neurons and oligodendrocyte lineage cells: Is it synaptic or non-synaptic? *Glia*, *67*(11), 2071–2091. <https://doi.org/10.1002/glia.23617>
- Li, C., Xiao, L., Liu, X., Yang, W., Shen, W., Hu, C., Yang, G., & He, C. (2013). A functional role of NMDA receptor in regulating the differentiation of oligodendrocyte precursor cells and remyelination. *Glia*, *61*(5), 732–749. <https://doi.org/10.1002/glia.22469>
- Lundgaard, I., Lzhynskaya, A., Stockley, J. H., Wang, Z., Evans, K. A., Swire, M., Volbracht, K., Gautier, H. O. B., Franklin, R. J. M., French-Constant, C., Attwell, D., & Káradóttir, R. T. (2013). Neuregulin and BDNF induce a Switch to NMDA receptor-dependent myelination by oligodendrocytes. *PLoS Biology*, *11*(12), e1001743. <https://doi.org/10.1371/journal.pbio.1001743>
- Luyt, K., Váradi, A., Durant, C. F., & Molnár, E. (2006). Oligodendroglial metabotropic glutamate receptors are developmentally regulated and involved in the prevention of apoptosis. *Journal of Neurochemistry*, *99*(2), 641–656. <https://doi.org/10.1111/j.1471-4159.2006.04103.x>
- Luyt, K., Váradi, A., & Molnár, E. (2003). Functional metabotropic glutamate receptors are expressed in oligodendrocyte progenitor cells. *Journal of Neurochemistry*, *84*(6), 1452–1464. <https://doi.org/10.1046/j.1471-4159.2003.01661.x>
- MacDonald, R. B., Kashikar, N. D., Lagnado, L., & Harris, W. A. (2017). A novel tool to measure extracellular glutamate in the zebrafish nervous system in vivo. *Zebrafish*, *14*(3), 284–286. <https://doi.org/10.1089/zeb.2016.1385>
- Marvin, J. S., Borghuis, B. G., Tian, L., Cichon, J., Harnett, M. T., Akerboom, J., Gordus, A., Renninger, S. L., Chen, T. W., Bargmann, C. I., Orger, M. B., Schreier, E. R., Demb, J. B., Gan, W. B., Hires, S. A., & Looger, L. L. (2013). An optimized fluorescent probe for visualizing glutamate neurotransmission. *Nature Methods*, *10*(2), 162–170. <https://doi.org/10.1038/nmeth.2333>
- Matthews, C. C., Zielke, H. R., Parks, D. A., & Fishman, P. S. (2003). Glutamate-pyruvate transaminase protects against glutamate toxicity in hippocampal slices. *Brain Research*, *978*(1–2), 59–64. [https://doi.org/10.1016/S0006-8993\(03\)02765-3](https://doi.org/10.1016/S0006-8993(03)02765-3)
- Matthews, C. C., Zielke, H. R., Wollack, J. B., & Fishman, P. S. (2000). Enzymatic degradation protects neurons from glutamate excitotoxicity. *Journal of Neurochemistry*, *75*(3), 1045–1052. <https://doi.org/10.1046/j.1471-4159.2000.0751045.x>
- Mensch, S., Baraban, M., Almeida, R., Czopka, T., Ausborn, J., El Manira, A., & Lyons, D. A. (2015). Synaptic vesicle release regulates myelin sheath number of individual oligodendrocytes in vivo. *Nature Neuroscience*, *18*(5), 628–630. <https://doi.org/10.1038/nn.3991>
- Micu, I., Plemel, J. R., Caprariello, A. V., Nave, K. A., & Stys, P. K. (2018). Axo-myelinic neurotransmission: A novel mode of cell signalling in the central nervous system. *Nature Reviews Neuroscience*, *19*(1), 49–58. <https://doi.org/10.1038/nrn.2017.128>
- Micu, I., Plemel, J. R., Lachance, C., Proft, J., Jansen, A. J., Cummins, K., van Minnen, J., & Stys, P. K. (2016). The molecular physiology of the axo-myelinic synapse. *Experimental Neurology*, *276*, 41–50. <https://doi.org/10.1016/j.expneurol.2015.10.006>

- Milner, R., Frost, E., Nishimura, S., Delcommenne, M., Streuli, C., Pytela, R., & ffrench-Constant, C. (1997). Expression of  $\alpha\text{v}\beta 3$  and  $\alpha\text{v}\beta 8$  integrins during oligodendrocyte precursor differentiation in the presence and absence of axons. *Glia*, 21(4), 350–360. [https://doi.org/10.1002/\(sici\)1098-1136\(199712\)21:4<350:aid-glia2>3.3.co;2-g](https://doi.org/10.1002/(sici)1098-1136(199712)21:4<350:aid-glia2>3.3.co;2-g)
- Mount, C. W., & Monje, M. (2017). Wrapped to adapt: Experience-dependent myelination. *Neuron*, 95(4), 743–756. <https://doi.org/10.1016/j.neuron.2017.07.009>
- Münzel, E. J., Schaefer, K., Obirei, B., Kremmer, E., Burton, E. A., Kuscha, V., Becker, C. G., Brösamle, C., Williams, A., & Becker, T. (2012). Claudin k is specifically expressed in cells that form myelin during development of the nervous system and regeneration of the optic nerve in adult zebrafish. *Glia*, 60(2), 253–270. <https://doi.org/10.1002/glia.21260>
- Nagarajan, B., Harder, A., Japp, A., Häberlein, F., Mingardo, E., Kleinert, H., Yilmaz, Ö., Zoons, A., Rau, B., Christ, A., Kubitscheck, U., Eiberger, B., Sandhoff, R., Eckhardt, M., Hartmann, D., & Odermatt, B. (2020). CNS myelin protein 36K regulates oligodendrocyte differentiation through Notch. *Glia*, 68(3), 509–527. <https://doi.org/10.1002/glia.23732>
- Nagy, B., Hovhannisyanyan, A., Barzan, R., Chen, T. J., & Kukley, M. (2017). Different patterns of neuronal activity trigger distinct responses of oligodendrocyte precursor cells in the corpus callosum. *PLoS Biology*, 15(8), e2001993. <https://doi.org/10.1371/journal.pbio.2001993>
- Ni, Q., Mehta, S., & Zhang, J. (2018). Live-cell imaging of cell signaling using genetically encoded fluorescent reporters. *FEBS Journal*, 285(2), 203–219. <https://doi.org/10.1111/febs.14134>
- Ortiz, F. C., Habermacher, C., Graciarena, M., Houry, P. Y., Nishiyama, A., Oumesmar, B. N., & Angulo, M. C. (2019). Neuronal activity in vivo enhances functional myelin repair. *JCI Insight*, 4(9). <https://doi.org/10.1172/jci.insight.123434>
- Pitt, D., Werner, P., & Raine, C. S. (2000). Glutamate excitotoxicity in a model of multiple sclerosis. *Nature Medicine*, 6(1), 67–70. <https://doi.org/10.1038/71555>
- Saab, A. S., Tzvetavona, I. D., Trevisiol, A., Baltan, S., Dibaj, P., Kusch, K., Möbius, W., Goetze, B., Jahn, H. M., Huang, W., Steffens, H., Schomburg, E. D., Pérez-Samartín, A., Pérez-Cerdá, F., Bakhtiari, D., Matute, C., Löwel, S., Griesinger, C., Hirrlinger, J., ... Nave, K.-A. (2016). Oligodendroglial NMDA Receptors Regulate Glucose Import and Axonal Energy Metabolism. *Neuron*, 91(1), 119–132. <https://doi.org/10.1016/j.neuron.2016.05.016>
- Sahel, A., Ortiz, F. C., Kerninon, C., Maldonado, P. P., Angulo, M. C., & Nait-Oumesmar, B. (2015). Alteration of synaptic connectivity of oligodendrocyte precursor cells following demyelination. *Frontiers in Cellular Neuroscience*, 9. <https://doi.org/10.3389/fncel.2015.00077>
- Schmidt, C., Ohlemeyer, C., Labrakakis, C., Walter, T., Kettenmann, H., & Schnitzer, J. (1997). Analysis of motile oligodendrocyte precursor cells in vitro and in brain slices. *Glia*, 20(4), 284–298. [https://doi.org/10.1002/\(SICI\)1098-1136\(199708\)20:4<284:AID-GLIA2>3.0.CO;2-6](https://doi.org/10.1002/(SICI)1098-1136(199708)20:4<284:AID-GLIA2>3.0.CO;2-6)
- Sheldon, A. L., & Robinson, M. B. (2007). The role of glutamate transporters in neurodegenerative diseases and potential opportunities for intervention. *Neurochemistry International*, 51(6-7), 333–355. <https://doi.org/10.1016/j.neuint.2007.03.012>
- Simpson, P. B., & Armstrong, R. C. (1999). Intracellular signals and cytoskeletal elements involved in oligodendrocyte progenitor migration. *Glia*, 26(1), 22–35. [https://doi.org/10.1002/\(SICI\)1098-1136\(199903\)26:1<22:AID-GLIA3>3.0.CO;2-M](https://doi.org/10.1002/(SICI)1098-1136(199903)26:1<22:AID-GLIA3>3.0.CO;2-M)
- Spitzer, S., Volbracht, K., Lundgaard, I., & Káradóttir, R. T. (2016). Glutamate signalling: A multifaceted modulator of oligodendrocyte lineage cells in health and disease. *Neuropharmacology*, 110, 574–585. <https://doi.org/10.1016/j.neuropharm.2016.06.014>
- Taveggia, C., Thaker, P., Petrylak, A., Caporaso, G. L., Toews, A., Falls, D. L., Einheber, S., & Salzer, J. L. (2008). Type III neuregulin-1 promotes oligodendrocyte myelination. *Glia*, 56(3), 284–293. <https://doi.org/10.1002/glia.20612>
- Tognatta, R., & Miller, R. H. (2016). Contribution of the oligodendrocyte lineage to CNS repair and neurodegenerative pathologies. *Neuropharmacology*, 110, 539–547. <https://doi.org/10.1016/j.neuropharm.2016.04.026>
- Trump, B. F., & Berezesky, I. K. (1996). Calcium-mediated cell injury and cell death. *The FASEB Journal*, 9(2), 219–228. <https://doi.org/10.1096/fasebj.9.2.7781924>
- Tsai, H. H., Macklin, W. B., & Miller, R. H. (2006). Netrin-1 is required for the normal development of spinal cord oligodendrocytes. *Journal of Neuroscience*, 26(7), 1913–1922. <https://doi.org/10.1523/JNEUROSCI.3571-05.2006>
- Valenti, O., Marino, M. J., Wittmann, M., Lis, E., DiLella, A. G., Kinney, G. G., & Conn, P. J. (2003). Group III metabotropic glutamate receptor-mediated modulation of the striatopallidal synapse. *Journal of Neuroscience*, 23(18), 7218–7226. <https://doi.org/10.1523/JNEUROSCI.23-18-07218.2003>
- Wake, H., Lee, P. R., & Fields, R. D. (2011). Control of local protein synthesis and initial events in myelination by action potentials. *Science*, 333(6049), 1647–1651. <https://doi.org/10.1126/science.1206998>
- Wake, H., Ortiz, F. C., Woo, D. H., Lee, P. R., Angulo, M. C., & Fields, R. D. (2015). Nonsynaptic junctions on myelinating glia promote preferential myelination of electrically active axons. *Nature Communications*, 6(7844). <https://doi.org/10.1038/ncomms8844>
- Weinreich, D., & Hammerschlag, R. (1975). Nerve impulse-enhanced release of amino acids from non-synaptic regions of peripheral and central nerve trunks of bullfrog. *Brain Research*, 84(1), 137–142. [https://doi.org/10.1016/0006-8993\(75\)90807-0](https://doi.org/10.1016/0006-8993(75)90807-0)
- Westerfield, M. (2007). *The zebrafish book. A guide for the laboratory use of zebrafish (Danio rerio)* (5th ed.). University of Oregon Press, Eugene (Book).
- Xiao, J., Wong, A. W., Willingham, M. M., Van Den Buuse, M., Kilpatrick, T. J., & Murray, S. S. (2011). Brain-derived neurotrophic factor promotes central nervous system myelination via a direct effect upon oligodendrocytes. *Neurosignals*, 18(3), 186–202. <https://doi.org/10.1159/000323170>
- Xin, W., Mironova, Y. A., Shen, H., Marino, R. A. M., Waisman, A., Lamers, W. H., Bergles, D. E., & Bonci, A. (2019). Oligodendrocytes support neuronal glutamatergic transmission via expression of glutamine synthetase. *Cell Reports*, 27(8), 2262–2271.e5. <https://doi.org/10.1016/j.celrep.2019.04.094>
- Zannino, D. A., & Appel, B. (2009). Olig2<sup>+</sup> precursors produce abducens motor neurons and oligodendrocytes in the zebrafish hindbrain. *Journal of Neuroscience*, 29(8), 2322–2333. <https://doi.org/10.1523/JNEUROSCI.3755-08.2009>
- Ziskin, J. L., Nishiyama, A., Rubio, M., Fukaya, M., & Bergles, D. E. (2007). Vesicular release of glutamate from unmyelinated axons in white matter. *Nature Neuroscience*, 10(3), 321–330. <https://doi.org/10.1038/nn1854>

## SUPPORTING INFORMATION

Additional supporting information may be found online in the Supporting Information section.

**FIGURE S1** EGFP/iGluSnFR is detected by Western blot. Specific bands at ~70 kDa in iGluSnFR-expressing (+) 5 dpf zfl (upper panel) and adult brains (lower panel) but not in iGluSnFR-negative (-) zfl or brain tissue can be detected.  $\beta$ -actin-positive loading control for all zfl and brain tissue samples is running at ~40 kDa. The reason for the double band in iGluSnFR<sup>(+)</sup> zfl has not been addressed so far

**FIGURE S2** Protein expression of CldnK and 36K in zfl. Whole Western blot membranes from Figure 5c. CldnK protein expression was lower in iGluSnFR<sup>(+)</sup> zfl compared to littermate controls not

expressing iGluSnFR. Similarly, the expression of 36K was lower in larvae expressing iGluSnFR compared to nonexpressing iGluSnFR littermate controls. Loading control  $\beta$ -actin expression was similar in all samples

**FIGURE S3** Protein expression of CldnK, 36K and Mbpa in adult zf brain. Whole Western blot membranes from Figure 5c. CldnK protein expression was lower in iGluSnFR<sup>(+)</sup> zf brain compared to wt controls not expressing iGluSnFR. Similarly, the expression of 36K and especially Mbpa was lower in brain tissue of zf-expressing iGluSnFR compared to nonexpressing wt controls. Loading control  $\beta$ -actin expression was similar in all samples

**FIGURE S4** In situ protein expression of Mbpa and PcnA was reduced in iGluSnFR-expressing zebrafish larvae at 5 dpf. (a) DAB immunostaining of Mbpa in brains of iGluSnFR-expressing zfl (left) versus controls (right) under low 10x magnification (upper) and high 40x magnification (lower). (b) DAB staining of Mbpa in the spinal cords of iGluSnFR-expressing zebrafish larvae (left) versus littermate controls (right) under low 10x magnification (upper) and high 40x magnification (lower), showing low expression of mbpa in iGluSnFR<sup>(+)</sup> compared to iGluSnFR<sup>(-)</sup> zfl in brains (a) and spinal cords (b). (c) DAB immunostaining of the proliferation marker PcnA in brains of iGluSnFR-expressing zebrafish larvae (left) versus controls (right) under low 10x magnification (upper) and high 40x magnification (lower). (d) DAB staining of PcnA in spinal cords of iGluSnFR-expressing zfl (left) versus controls (right) under low 10x magnification (upper) and high 40x magnification (lower), showing less expression of PcnA in iGluSnFR<sup>(+)</sup> compared to iGluSnFR<sup>(-)</sup> larvae in brains (c) and spinal cords (d). (e) DAB immunostaining of the apoptosis marker CC3 in brains of iGluSnFR-expressing zebrafish larvae (left) versus controls (right) under low 10x magnification (upper) and high 40x magnification (lower). (f) DAB immunostaining of CC3 in spinal cords of iGluSnFR-expressing zebrafish larvae (left) versus littermate controls (right) under low 10x magnification (upper) and high 40x magnification (lower). Unlike Mbpa and PcnA, CC3 expression was generally very low and not clearly different between iGluSnFR-expressing zebrafish larvae (left) and littermate controls (right). Scale bars (0.2 mm)

**FIGURE S5** In situ expression of CldnK, 36K, and PcnA proteins was reduced in iGluSnFR-expressing adult zebrafish brains compared to controls: DAB staining of CldnK under 4x magnification (a, upper), 10x magnification (a, lower–b, upper) and 40x magnification (b, lower). CldnK expression was considerably reduced in iGluSnFR-expressing adult zebrafish brains versus wt controls. 36K and PcnA expressions were also diminished in iGluSnFR-expressing adult zebrafish brains compared to wt controls, as shown respectively in DAB immunostaining of adult zebrafish cerebellum sections (c and d) under

4x magnification (*in upper panels*: c for 36K and d for PcnA); and 10x magnification (*in corresponding lower panels*). Protein expression of the apoptosis marker CC3 in (e) did not obviously change in iGluSnFR-expressing adult zebrafish brains compared to wt controls. As expected, eGFP / iGluSnFR was detected by anti-EGFP immunostaining in iGluSnFR-expressing adult zf cerebellum (f, left); but not in WT adult zebrafish brains (f, right) under 4x (f, upper) and 10x magnification (f, lower). Scale bars: 500  $\mu$ m (a, b, c “upper”, d, e, f) and 50  $\mu$ m (c “lower”)

**FIGURE S6** The number of Olig2<sup>(+)</sup> dorsal OPCs and the OL marker CldnK was increased in iGluSnFR-expressing zebrafish at 5 dpf, after treatment with L-AP4. Example images referring to Figure 6b,c. (a) The number of Olig2<sup>(+)</sup> dorsal OPCs was increased (rescued) in iGluSnFR-expressing zebrafish at 5 dpf, after ventricle injections of L-AP4 at 3 dpf. Z-projections of proximal spinal cord regions in lateral view obtained from two-photon microscopy are shown. Each Z-stack had the same dimensions in x, y, and z and was obtained from approximately the same spinal cord region in the fish. The first left row (red) shows a considerably higher expression of Olig2<sup>(+)</sup> cells in L-AP4-injected iGluSnFR<sup>(-)</sup> larvae compared to Ctrl-injected group. Each row shows three representative samples. The iGluSnFR expression is shown in green in third and fourth row, corresponding to L-AP4- and Ctrl-injected groups, respectively. Scale bar: 50  $\mu$ m. (b) Low-resolution epi-fluorescence microscopic images of proximal zebrafish spinal cords in lateral view at 5 dpf. (b, upper) Treatment of 1mM L-AP4 shows a high expression of CldnK:mem-tdTomato (red, first left row) in zfl not expressing iGluSnFR, compared to Ctrl-injected and uninjected groups (middle and right row respectively). Each row shows three representative zfl samples. (b, lower) Treatment of 1mM L-AP4 results in a higher expression of CldnK:mem-tdTomato (red, first left row) in zfl expressing iGluSnFR, compared to Ctrl-injected (third row from left) and uninjected iGluSnFR<sup>(+)</sup> zfl groups (fifth row from left). iGluSnFR expression is similar in L-AP4-injected (green, second row from left), Ctrl-injected (green, fourth row from left), and uninjected groups (green, sixth row from left). Each row shows three representative samples. Scale bar: 50  $\mu$ m

Transparent Peer Review Report

Transparent Science Questionnaire for Authors

**How to cite this article:** Turan F, Yilmaz Ö, Schünemann L, et al. Effect of modulating glutamate signaling on myelinating oligodendrocytes and their development—A study in the zebrafish model. *J Neurosci Res.* 2021;00:1–19. <https://doi.org/10.1002/jnr.24940>